J. Fluid Mech. (1999), *vol.* 389, *pp.* 275–301. Printed in the United Kingdom

A consistent coupled-mode theory for the propagation of small-amplitude water waves over variable bathymetry regions

By G. A. ATHANASSOULIS AND K. A. BELIBASSAKIS

Department of Naval Architecture and Marine Engineering,
National Technical University of Athens, PO Box 64033 Zografos, 15710 Athens, Greece
e-mail: mathan@central.ntua.gr, kbel@fluid.mech.ntua.gr

(Received 20 December 1997 and in revised form 10 January 1999)

Extended mild-slope equations for the propagation of small-amplitude water waves over variable bathymetry regions, recently proposed by Massel (1993) and Porter & Staziker (1995), are shown to exhibit an inconsistency concerning the sloping-bottom boundary condition, which renders them non-conservative with respect to wave energy. In the present work, a consistent coupled-mode theory is derived from a variational formulation of the complete linear problem, by representing the vertical distribution of the wave potential as a uniformly convergent series of local vertical modes at each horizontal position. This series consists of the vertical eigenfunctions associated with the propagating and all evanescent modes and, when the slope of the bottom is different from zero, an additional mode, carrying information about the bottom slope. The coupled-mode system obtained in this way contains an additional equation, as well as additional interaction terms in all other equations, and reduces to the previous extended mild-slope equations when the additional mode is neglected. Extensive numerical results demonstrate that the present model leads to the exact satisfaction of the bottom boundary condition and, thus, it is energy conservative. Moreover, it is numerically shown that the rate of decay of the modal-amplitude functions is improved from $O(n^{-2})$, where n is the mode number, to $O(n^{-4})$, when the additional sloping-bottom mode is included in the representation. This fact substantially accelerates the convergence of the modal series and ensures the uniform convergence of the velocity field up to and including the boundaries.

1. Introduction

The interaction of free-surface gravity waves with uneven bottom topography in water of intermediate depth is a mathematically difficult problem, for which a broad class of approximation techniques has been developed. Although the nonlinear effects become significant as the shoreline is approached, a consistent linear solution is still very useful, providing a great deal of information concerning the wave field and its impact on the nearshore environment. In addition, linear theory serves as the starting point for any weakly nonlinear model. In this work, an enhanced coupled-mode formulation is derived, capable of treating the complete linear problem, without any simplifications concerning the vertical structure of the wave field, and without any assumptions concerning the bottom slope and curvature.

Theoretical aspects of the problem of small-amplitude water waves travelling in a region of varying depth, mainly uniqueness results, have been presented, under

various geometric assumptions, by Vainberg & Maz'ja (1973), Fitz-Gerald (1976), Fitz-Gerald & Grimshaw (1979), Simon & Ursell (1984), Kuznetsov (1991, 1993) and other authors. See also the survey by Evans & Kuznetsov (1997). Besides, general methods for direct numerical solution of the linear problem, such as finite-element methods, boundary-integral-equation methods or hybrid techniques are available; see, e.g. the surveys by Mei (1978, 1983), Euvrard *et al.* (1981), Yeung (1982), Porter & Chamberlain (1997). Moreover, general numerical techniques based on a topography discretization or on a domain transformation have been developed. See, e.g. Devillard, Dunlop & Souillard (1988), Rey (1992) for the former, and Evans & Linton (1994) for the latter approach. However, the computational cost of these generic techniques is high, rendering them inappropriate, especially for long-range propagation and/or in three dimensions. Owing to this fact, a constantly growing emphasis has been given on the development of approximate wave models retaining only the essential features of specific families of problems and, thus, being better suited for long-range wave propagation.

A well-known specific feature of water waves is that the propagation space does not coincide with the physical space. While the latter is the whole liquid domain (an irregularly shaped horizontal strip in the case of a shallow-sea environment), the former is only the horizontal direction(s). This fact, which is a manifestation of the surface (boundary) character of water waves, leads to the reformulation of the propagation problem as a non-local wave equation in the propagation (horizontal) space. In the linear case, on which we shall focus our attention in the present work, the appropriate non-local equation may take the form (in the time domain) of either an operator differential equation (Garipov 1965; Moiseev 1964; Moiseev & Rumiantsev 1968; Craig & Sulem 1993), or an integrodifferential equation (Fitz-Gerald 1976), or a pseudodifferential equation (Milder 1977; Miles 1977; Craig & Sulem 1993) or even a partial differential equation with respect to the complex-analytic wave potential (Athanassoulis & Makrakis 1994). Another possibility, which will be discussed in detail in the present work, is to reformulate the problem as an infinite system of horizontal equations with variable coefficients. A clear consequence of the non-local character of the water-wave problem in the propagation space is that any one-equation model (i.e. one differential equation in the horizontal direction(s)) cannot capture all features of the problem. Nevertheless, because of the complexity of the problem, a plethora of one-equation models have been proposed and studied, each one with its range of applicability and its advantages.

Historically, Eckart (1952) was the first author who proposed a one-equation model for intermediate-depth water. Berkhoff (1972, 1976) derived a slightly more general model, called the mild-slope equation. Both authors used predetermined vertical distributions of the wave potential and applied a depth averaging procedure in order to obtain equations in the propagation space. Other derivations of similar or improved one-equation models, using either averaging techniques or variational principles, have been given by Smith & Sprinks (1975), Lozano & Meyer (1976), Booij (1981), Radder & Dingemans (1985), Kirby (1986*a*, *b*), Massel (1993); see also the general surveys by Massel (1989), Mei (1983), Porter & Chamberlain (1997) and Dingemans (1997) and the many references cited there, as well as the paper by Miles (1991), where a thorough comparison between Eckart's and Berkhoff's models is made. In general, mild-slope equations can be considered satisfactory for mean bottom slopes up to 1 : 3 (Booij 1983; Berkhoff, Booij & Radder 1982) and some of them (the appropriately modified ones such as Kirby 1986*a*, *b*), can also predict the high backscattering due to Bragg resonance, occurring when an undulating component is superimposed on a

slowly varying bottom topography. (Bragg scattering has also been studied by using perturbation techniques by Davies & Heathershaw 1984, Mei 1985 and Hara & Mei 1987). Another important feature of most of the mild-slope models (but not Eckart's, Miles 1991) is that, despite their approximate character, they conserve wave energy.

The basic restriction inherent to any one-equation model is that the vertical structure of the wave field is given by a specific, preselected, depth function. This restriction makes them inappropriate to describe the wave field when the bottom topography is complicated and the depth is sufficiently small so that the velocity field interacts with the bottom. The improvement of the mild-slope models to match the requirements of this situation calls for a more general representation of the vertical structure of the wave field. Massel (1993) and Porter & Staziker (1995) presented this kind of model, called extended mild-slope equations, in which the vertical profile of the wave potential at any horizontal position is represented by a local-mode series involving the propagating and all evanescent modes. The amplitudes of the modes are unknown functions supported in the propagation space. Then, using either a Galerkin approach (Massel 1993) or a variational principle (Porter & Staziker 1995), an infinite set of coupled equations for the unknown amplitudes is obtained, which is called (by the present authors) the *coupled-mode system*. See also the survey by Porter & Chamberlain (1997). Similar coupled-mode systems have also been derived and extensively used in the context of hydroacoustics; see, e.g. Boyles (1984) and Fawcett (1992).

The local-mode vertical expansion of the wave potential used by Massel (1993) and Porter & Staziker (1995) consists of a forward and (possibly) a backward propagating mode plus the evanescent modes. All these modes are determined by the dispersion relation at the local depth; they satisfy the linearized free-surface condition and have zero vertical derivative at the local depth. Such a representation is complete for a flat or a piecewise flat bottom, and has been used for solving the water-wave propagation problem over a step (see, e.g. Newman 1965; Miles 1967; Mei & Black 1969) or a steplike bottom (Devillard *et al.* 1988; O'Hare & Davies 1992, 1993; Rey 1992). However, this expansion is inconsistent with the Neumann condition on a sloping bottom, since each of the vertical modes involved violates it and, thus, the solution, being a linear superposition of modes, behaves the same. This fact has two important consequences. First, the velocity field (normal and tangential velocities) in the vicinity of the bottom is poorly represented and, secondly, wave energy is not generally conserved. This situation, which is discussed in detail in § 4, is remedied in the present work by including in the standard representation of the wave potential an additional term, called the *sloping-bottom mode*.

The present work is structured as follows. In § 2 the complete, linearized, boundary-value problem is considered in the frequency domain. Since the water layer extends to infinity in the horizontal directions, the assumption is made that, in the far field, the depth is eventually constant (although may be different in different directions). The problem is formulated as a transmission problem in the finite subdomain of varying bathymetry, closed by the appropriate matching conditions at the vertical interfaces. In § 3, a variational formulation of the hydrodynamic problem is presented. In § 4 a complete representation of the velocity potential, to be used in conjuction with the variational principle, is developed. After discussing the deficiencies of the standard local-mode representations, an enhanced representation is given, including the standard set of modes (propagating and evanescent) and an additional mode (the sloping-bottom mode), enabling the exact satisfaction of the bottom boundary condition and, as a consequence, the conservation of wave energy. Subsequently, in § 5, a coupled-mode system of horizontal equations, along with an appropriate

set of boundary conditions, are derived by applying the variational principle to the enhanced representation of the wave potential. The obtained coupled-mode system differs from the ones given previously by other authors in two respects. First, an additional equation appears, corresponding to the unknown amplitude of the sloping-bottom mode and, secondly, additional terms enter all equations, describing the interaction between the sloping-bottom and the other modes. In § 6 the approximate solution of the problem is obtained by truncating the enhanced local-mode series into a finite number of terms, retaining the propagating, the sloping-bottom and a sufficient number of evanescent modes required to achieve numerical convergence. Numerical results are presented for three different environments showing that the numerical convergence of the enhanced series, as compared to the standard ones, is substantially improved. Moreover, with the aid of a systematic numerical investigation, it is found that the rate of decay of the modal-amplitude functions is improved from $O(n^{-2})$, where n is the mode number, to $O(n^{-4})$, when the sloping-bottom mode is included in the representation. Thus, in most practical applications, a small number of modes with the enhanced representation is sufficient to accurately calculate the velocity field up to (and including) the boundaries.

A feature of the enhanced coupled-mode theory presented in this work is that, being equivalent to the complete linearized problem, it can be naturally reduced to mild-slope models in subareas where the physical conditions permit it. In this sense, the present method shares characteristics of both a top-down approach, ensuring completeness and consistency, and a bottom-up approach, letting the user to go back up to a very simple one-equation model, saving computational time.

2. Differential formulation of the problem

The studied marine environment consists of a water layer D_{3D} bounded above by the free surface $\partial D_{F,3D}$ and below by a rigid bottom $\partial D_{\Pi,3D}$. It is assumed that the bottom slope exhibits an arbitrary one-dimensional variation in a subdomain of finite length, i.e. the bathymetry is characterized by parallel, straight bottom contours lying between two regions of constant but different depth, $h = h_1$ (region of incidence) and $h = h_3$ (region of transmission); see figure 1. The liquid is assumed to be homogeneous, inviscid and incompressible. The wave field is excited by an incident monochromatic plane wave, propagating with direction normal to the bottom contours. The characteristic lengthscales involved (directly or indirectly) in the above problem are: the two far-field water depths h_i, $i = 1, 3$, the corresponding far-field wave lengths λ_i, $i = 1, 3$, the bottom variation length, as well as an average amplitude of bottom corrugations. From these characteristic lengths we can form various non-dimensional characteristic numbers, the most important of which are: The shallowness ratios h_i/λ_i, $i = 1, 3$, the mean and the maximum bottom slopes s_{mean}, s_{max}, and the shoaling ratio h_3/h_1. In the present work, all these non-dimensional numbers are considered to be of the same order of magnitude. That is, no asymptotic assumptions are made for them.

Before proceeding to the formulation of the problem, we shall introduce some geometrical notation. A Cartesian coordinate system is introduced, with its origin at some point on the mean water level (in the variable bathymetry region), the z-axis pointing upwards and the y-axis being parallel to the bottom contours. See figure 1. The liquid domain D_{3D} will be represented by $D_{3D} = D \times R$, where D is the (two-dimensional) intersection of D_{3D} by a vertical plane perpendicular to the bottom

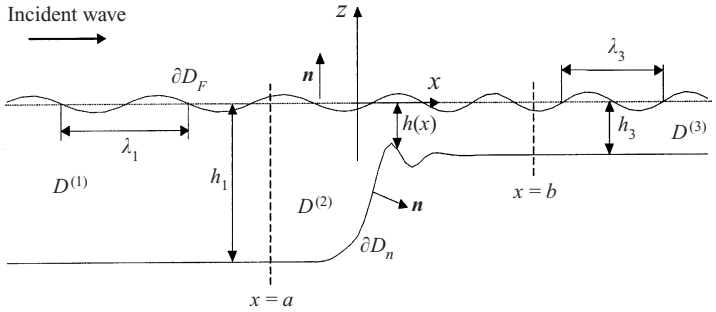

FIGURE 1. Domain decomposition and basic notation.

contours, and $R = (-\infty, +\infty)$ is a copy of the real line:

$$D_{3D} = \{(x, y, z) : \ (x, y) \in R^2, -h(x) < z < 0\}, \quad D = \{(x, z) : \ x \in R, -h(x) < z < 0\}. \tag{2.1}$$

The function $h(x)$, appearing in the above definitions, represents the local depth, measured from the mean water level. It is considered to be a twice continuously differentiable function defined on the real axis R, such that

$$h(x) = h(a) = h_1 \quad \text{for all } x \leqslant a, \quad h(x) = h(b) = h_3 \quad \text{for all } x \geqslant b. \tag{2.2}$$

The liquid domain D_{3D} is decomposed in three subdomains $D_{3D}^{(i)} = D^{(i)} \times R$, $i = 1, 2, 3$, defined as follows: $D_{3D}^{(1)}$ is the constant-depth subdomain characterized by $x < a$, $D_{3D}^{(3)}$ is the constant-depth subdomain characterized by $x > b$, and $D_{3D}^{(2)}$ is the variable bathymetry subdomain lying between $D_{3D}^{(1)}$ and $D_{3D}^{(3)}$. Without loss of generality, we assume that $h_1 > h_3$. The decomposition is also applied to the boundaries $\partial D_{F,3D} = \partial D_F \times R$ and $\partial D_{\Pi,3D} = \partial D_\Pi \times R$. The lines ∂D_F and ∂D_Π are decomposed in three pieces each, for example, $\partial D_F = \partial D_F^{(1)} \cup \partial D_F^{(2)} \cup \partial D_F^{(3)}$, where $\partial D_F^{(1)}$ belongs to the boundary of $D^{(i)}$, and similarly for ∂D_Π. Finally, we define the vertical interfaces $\partial D_{1,3D}^{(12)} = \partial D_I^{(12)} \times R$ and $\partial D_{I,3D}^{(23)} = \partial D_I^{(23)} \times R$, which are the common vertical boundaries of subdomains $D_{3D}^{(1)}$ and $D_{3D}^{(2)}$, and $D_{3D}^{(2)}$ and $D_{3D}^{(3)}$, respectively. Clearly, $\partial D_I^{(12)}$ and $\partial D_I^{(23)}$ are vertical segments (between the bottom and the mean water level) at $x = a$ and $x = b$, respectively. See figure 1.

Assuming that the free-surface elevation and the velocity field are small enough, the linearized water-wave equations can be used. See, e.g. Stoker (1957) or Wehausen & Laitone (1960) or Mei (1983). Then, the velocity field is time harmonic with angular frequency ω, the same as the incident wave, and can be represented by a velocity potential of the form

$$\Phi(x, z; t) = \mathrm{Re}\left\{-\frac{\mathrm{i}gH}{2\omega}\varphi(x, z; \mu)\, \exp(-\mathrm{i}\omega t)\right\}, \tag{2.3}$$

where H is the incident wave height, g is the acceleration due to gravity, $\mu = \omega^2/g$ is the frequency parameter, and $\mathrm{i} = \sqrt{-1}$. The function $\varphi = \varphi(x, z; \mu)$ appearing in (2.3), is the normalized potential in the frequency domain, usually written as $\varphi(x, z)$. The problem of water-wave propagation over the variable bathymetry region can be formulated as a transmission problem in the bounded subdomain $D^{(2)}$, with the aid of

the following general representation of the wave potential $\varphi(x,z)$ in the semi-infinite strips $D^{(1)}$ and $D^{(3)}$ (see e.g. Miles 1967; Mei & Black 1969; Massel 1993):

$$\varphi^{(1)}(x,z) = (A_0 \exp(\mathrm{i}k_0^{(1)}x) + A_R \exp(-\mathrm{i}k_0^{(1)}x))Z_0^{(1)}(z) + \sum_{n=1}^{\infty} C_n^{(1)} Z_n^{(1)}(z) \exp(k_n^{(1)}(x-a)) \quad ((x,z) \in D^{(1)}) \tag{2.4}$$

$$\varphi^{(3)}(x,z) = A_T \exp(\mathrm{i}k_0^{(3)}x) Z_0^{(3)}(z) + \sum_{n=1}^{\infty} C_n^{(3)} Z_n^{(3)}(z) \exp(k_n^{(3)}(b-x)) \quad ((x,z) \in D^{(3)}). \tag{2.5}$$

The terms $(A_0 \exp(\mathrm{i}k_0^{(1)}x) + A_R \exp(-\mathrm{i}k_0^{(1)}x))Z_0^{(1)}(z)$ and $A_T \exp(\mathrm{i}k_0^{(3)}x)Z_0^{(3)}(z)$ in the series (2.4) and (2.5), respectively, are the propagating modes, whereas the remaining ones ($n = 1,2,\ldots$) are the evanescent modes. In the expansions (2.4) and (2.5), the sets of numbers $\{\mathrm{i}k_0^{(i)}, k_n^{(i)}, n = 1,2,\ldots\}$, $i = 1,3$, and the sets of vertical functions $\{Z_n^{(i)}(z),\ n = 0,1,2,\ldots\}$, $i = 1,3$, are the eigenvalues and the corresponding eigenfunctions of the regular Sturm–Liouville problems obtained by separation of variables in the half-strips $D^{(i)}, i = 1,3$. The eigenvalues $\{\mathrm{i}k_0^{(i)}, k_n^{(i)}\}$ are given as the roots of the dispersion relations

$$\mu h_i = -k^{(i)} h_i \tan(k^{(i)} h_i) \quad (i = 1,3), \tag{2.6}$$

and the eigenfunctions $\{Z_n^{(i)}(z), n = 0,1,2,\ldots\}$ are given by

$$Z_0^{(i)}(z) = \frac{\cosh(k_0^{(i)}(z+h_i))}{\cosh(k_0^{(i)}h_i)}, \quad Z_n^{(i)}(z) = \frac{\cos(k_n^{(i)}(z+h_i))}{\cos(k_n^{(i)}h_i)}, \quad (n = 1,2,\ldots, \quad i = 1,3). \tag{2.7}$$

The correctness (completeness) of the expansions (2.4) and (2.5) follows by the standard theory of regular eigenvalue problems. See, e.g. Coddington & Levinson (1955 § 7.4).

Given the coefficient A_0 of the incident wave, the half-strip potentials $\varphi^{(1)}$ and $\varphi^{(3)}$ are uniquely determined by means of the complex coefficients $A_R, \{C_n^{(1)}\}_{n\in N}$ and A_T, $\{C_n^{(3)}\}_{n\in N}$, respectively; see (2.4) and (2.5). Bearing this in mind, we shall occasionally use the notation:

$$\varphi^{(1)} = \varphi^{(1)}(x,z;\ A_R, \{C_n^{(1)}t\}_{n\in N}), \quad \varphi^{(3)} = \varphi^{(3)}(x,z;\ A_T, \{C_n^{(3)}\}_{n\in N}).$$

When we are interested in the parametric dependence of the half-strip potentials on the coefficients $A_R, \{C_n^{(1)}\}_{n\in N}$ and $A_T, \{C_n^{(3)}\}_{n\in N}$, the field-point variables (x,z) will be omitted.

By exploiting the representations (2.4) and (2.5), the problem can be formulated as a transmission boundary-value problem in the bounded subdomain $D^{(2)}$, as follows:

PROBLEM $\mathscr{P}_T(D^{(2)}, \mu, A_0)$. *Given the constants* $A_0 = \exp(\mathrm{i}\theta_0)$ *and* $\mu = \omega^2/g > 0$, *and the representations* (2.4) *and* (2.5) *of the wave potential in the semi-infinite strips* $D^{(1)}$ *and* $D^{(3)}$, *find the coefficients* $A_R, \{C_n^{(1)}\}_{n\in N}$ *and* $A_T, \{C_n^{(3)}\}_{n\in N}$, *and the function* $\varphi^{(2)}(x,z)$, *defined in* $D^{(2)}$, *satisfying the following system of equations, boundary and*

matching conditions:

$$\nabla^2\varphi^{(2)} = 0 \quad ((x,z) \in D^{(2)}), \tag{2.8a}$$

$$\frac{\partial\varphi^{(2)}}{\partial n^{(2)}} - \mu\varphi^{(2)} = 0, \quad (x,z) \in \partial D_F^{(2)}, \quad \frac{\partial\varphi^{(2)}}{\partial n^{(2)}} = 0 \quad ((x,z) \in \partial D_H^{(2)}), \tag{2.8b,c}$$

$$\varphi^{(2)} = \varphi^{(1)}, \quad \frac{\partial\varphi^{(2)}}{\partial n^{(2)}} = -\frac{\partial\varphi^{(1)}}{\partial n^{(1)}} \quad ((x,z) \in \partial D_I^{(12)}), \tag{2.8d,e}$$

$$\varphi^{(2)} = \varphi^{(3)}, \quad \frac{\partial\varphi^{(2)}}{\partial n^{(2)}} = -\frac{\partial\varphi^{(3)}}{\partial n^{(3)}} \quad ((x,z) \in \partial D_I^{(23)}), \tag{2.8f,g}$$

where $n^{(i)} = (n_x^{(i)}, n_z^{(i)})$ *is the unit normal vector to the boundary* $\partial D^{(i)}$ *directed to the exterior of* $D^{(i)}$, $i = 1, 2, 3$.

The problem (2.8*a–g*) will be referred to as *the transmission problem* $\mathscr{P}_T(D^{(2)}, \mu, A_0)$. This problem admits of an equivalent variational formulation; see, e.g. Bai & Yeung (1974), Mei & Chen (1975, 1976), Mei (1978), Aranha, Mei & Yue (1979). The variational principle will be presented in the next section, and will serve as the basis for the derivation of the enhanced coupled-mode system of horizontal equations.

3. Variational formulation of the problem

Consider the functional:

$$\begin{aligned}
&\mathscr{F}(\varphi^{(2)}, A_R, \{C_n^{(1)}\}_{n\in N}, A_T, \{C_n^{(3)}\}_{n\in N}) \\
&\quad = \frac{1}{2}\int_{D^{(2)}} (\nabla\varphi^{(2)})^2 \mathrm{d}V - \tfrac{1}{2}\mu \int_{\partial D_I^{(2)}} (\varphi^{(2)})^2 \mathrm{d}S \\
&\qquad + \int_{\partial D_I^{(12)}} (\varphi^{(2)} - \tfrac{1}{2}\varphi^{(1)}(A_R, \{C_n^{(1)}\}_{n\in N})) \frac{\partial\varphi^{(1)}(A_R, \{C_n^{(1)}\}_{n\in N})}{\partial n^{(1)}} \mathrm{d}S \\
&\qquad + \int_{\partial D_I^{(23)}} (\varphi^{(2)} - \tfrac{1}{2}\varphi^{(3)}(A_T, \{C_n^{(3)}\}_{n\in N})) \frac{\partial\varphi^{(3)}(A_T, \{C_n^{(3)}\}_{n\in N})}{\partial n^{(3)}} \mathrm{d}S - A_0 A_R J^{(1)},
\end{aligned} \tag{3.1}$$

where $J^{(1)}$ is a constant defined by the equation

$$J^{(1)} = 2k_0^{(1)} \int_{z=-h_1}^{z=0} (Z_0^{(1)}(z))^2 \mathrm{d}z. \tag{3.2}$$

The variational formulation of the problem $\mathscr{P}_T(D^{(2)}, \mu, A_0)$ is now stated as follows:

THEOREM 1 [*The variational principle*]. *The function* $\varphi^{(2)}(x,z), (x,z) \in D^{(2)}$ *and the coefficients* $A_R, \{C_n^{(1)}\}_{n\in N}$ *and* $A_T, \{C_n^{(3)}\}_{n\in N}$ *constitute a solution of the problem* $\mathscr{P}_T(D^{(2)}, \mu, A_0)$ *if and only if they render the functional* $\mathscr{F}$, *equation* (3.1), *stationary, i.e.*

$$\delta\mathscr{F}(\varphi^{(2)}, A_R, \{C_n^{(1)}\}, A_T, \{C_n^{(3)}\}) = 0. \tag{3.3a}$$

Proof. By calculating the first variation $\delta\mathscr{F}$ of the functional (see, e.g. Bai & Yeung 1974 or Mei & Chen 1975), the variational equation (3.3*a*) takes the form:

$$-\int_{D^{(2)}}\left(\nabla^2\varphi^{(2)}\right)\delta\varphi^{(2)}\mathrm{d}V+\int_{\partial D_{\Pi}^{(2)}}\left(\frac{\partial\varphi^{(2)}}{\partial n^{(2)}}\right)\delta\varphi^{(2)}\mathrm{d}S+\int_{\partial D_{I}^{(2)}}\left[\frac{\partial\varphi^{(2)}}{\partial n^{(2)}}-\mu\varphi^{(2)}\right]\delta\varphi^{(2)}\mathrm{d}S$$
$$+\int_{\partial D_{I}^{(12)}}\left(\frac{\partial\varphi^{(2)}}{\partial n^{(2)}}+\frac{\partial\varphi^{(1)}}{\partial n^{(1)}}\right)\delta\varphi^{(2)}\mathrm{d}S+\int_{\partial D_{I}^{(23)}}\left(\frac{\partial\varphi^{(2)}}{\partial n^{(2)}}+\frac{\partial\varphi^{(3)}}{\partial n^{(3)}}\right)\delta\varphi^{(2)}\mathrm{d}S$$
$$+\int_{\partial D_{I}^{(12)}}\left(\varphi^{(2)}-\varphi^{(1)}\right)\delta\left(\frac{\partial\varphi^{(1)}}{\partial x}\right)\mathrm{d}S-\int_{\partial D_{I}^{(23)}}\left(\varphi^{(2)}-\varphi^{(3)}\right)\delta\left(\frac{\partial\varphi^{(3)}}{\partial x}\right)\mathrm{d}S=0. \quad (3.3b)$$

The two functions $\partial\varphi^{(i)}/\partial x$, $i=1,3$, appearing in the last two terms, are considered to be represented by means of their series expansions obtained by differentiating (2.4) and (2.5). Consequently, the variations $\delta(\partial\varphi^{(1)}/\partial x)$ and $\delta(\partial\varphi^{(3)}/\partial x)$ are, eventually, expressed in terms of the variations of the coefficients $\delta A_R, \{\delta C_n^{(1)}\}_{n\in N}$ and $\delta A_T, \{\delta C_n^{(3)}\}_{n\in N}$, respectively.

The proof of the equivalence of the variational equation (3.3*b*) and the problem $\mathscr{P}_T(D^{(2)},\mu,A_0)$ is completed by using standard arguments of calculus of variations (e.g. Gelfand & Fomin 1963, ch. 36, or Rektorys 1977, ch. 22). It is based on the arbitrariness of variations of the potential field

$$\delta\varphi^{(2)}\text{ in }D^{(2)},\quad \delta\varphi^{(2)}\text{ on }\partial D_{\Pi}^{(2)},\quad \delta\varphi^{(2)}\text{ on }\partial D_{F}^{(2)},\quad \delta\varphi^{(2)}\text{ on }\partial D_{I}^{(12)},\quad \delta\varphi^{(2)}\text{ on }\partial D_{I}^{(23)},$$

and of the coefficients of the left- and the right-strip expansions

$$\delta A_R,\quad \delta C_n^{(1)},\quad \delta A_T,\quad \delta C_n^{(3)}\quad (n=1,2,\ldots),$$

in conjunction with the fact that the systems $\{Z_n^{(i)}(z)\}_{n\in N}$ are complete in the intervals $(-h_i,0)$, $i=1,3$, respectively.

Apart from its theoretical interest, the usefulness of the above variational principle hinges on the fact that it leaves us the freedom to choose any particular representation for the unknown potential $\varphi^{(2)}$ in $D^{(2)}$. In this way, a variety of possible algorithms for the numerical solution of the wave problem at hand can be constructed. One possible choice, enabling the treatment of water-wave problems in marine environments without restrictions as regards the bottom slope or curvature, will be presented in the following section.

4. Local mode representations of the wave potential in the variable bathymetry region

4.1. *The standard representation and its deficiencies*

We shall now present and discuss a specific representation of the wave potential $\varphi^{(2)}(x,z)$ in the variable bathymetry subdomain $D^{(2)}$, following the lines of thought that were first introduced by Pierce (1965) in the context of ocean acoustics. Since then, this technique has been used extensively in the context of hydroacoustics (e.g. Boyles 1984; Fawcett 1992) and, recently, in water waves (Massel 1993; Porter & Staziker 1995; Porter & Chamberlain 1997).

Given the depth function $h(x)$, $x\in R$, and the wave parameter $\mu=\omega^2/g>0$, we are able to formulate and solve the local dispersion relation at every $x\in[a,b]$:

$$\mu h(x)=-k(x)h(x)\tan[k(x)h(x)]\quad (a\leqslant x\leqslant b), \quad (4.1)$$

obtaining, thus, the local eigenvalues $\{ik_0(x), k_n(x), n = 1, 2, \ldots\}$, and the local vertical eigenfunctions

$$Z_0(z;x) = \frac{\cosh[k_0(x)(z+h(x))]}{\cosh(k_0(x)h(x))}, \quad Z_n(z;x) = \frac{\cos[k_n(x)(z+h(x))]}{\cos(k_n(x)h(x))} \quad (n = 1, 2\ldots). \tag{4.2}$$

The above eigenvalues and eigenfunctions constitute the solution of the following local vertical Sturm–Liouville problem:

$$\frac{\partial^2 Z(z;x)}{\partial z^2} + (k(x))^2 Z(z;x) = 0 \quad (-h(x) < z > 0), \tag{4.3a}$$

$$\frac{\partial Z(0;x)}{\partial z} - \mu Z(0;x) = 0 \quad \left(\frac{\partial Z(-h(x);x)}{\partial z} = 0\right). \tag{4.3b,c}$$

It should be noted here that, in the above equations, the dependence on the horizontal position x is of a parametric nature. Consequently, the Sturm–Liouville problem, equations (4.3), should be considered as a family of problems, each one corresponding to each value of the parameter x. The characterizations local eigenvalues and local eigenfunctions are used in order to emphasize this fact. On the basis of the general theory of Sturm–Liouville problems (e.g. Titchmarsh 1962 ch. 1; Higgins 1977 ch. 4), the set of z-functions $\{Z_n(z;x)\}_{n=0,1,\ldots}$ constitutes a complete orthogonal system in $L^2(-h(x), 0)$, for each value of $x \in [a, b]$. Accordingly, the following L^2 -representation of the (unknown) wave potential $\varphi^{(2)}$ in $D^{(2)}$ can be considered:

$$\varphi^{(2)}(x,z) = \varphi_0(x)Z_0(z;x) + \sum_{n=1}^{\infty} \varphi_n(x)Z_n(z;x), \tag{4.4}$$

where $\varphi_n(x), n = 0, 1, 2, \ldots$, are the coefficients of the generalized Fourier expansion of $\varphi^{(2)}(x,z)$ with respect to the L^2-basis $Z_n(z;x)$, $n = 0, 1, 2, \ldots$, for each $x \in [a, b]$. This representation of the wave potential $\varphi^{(2)}$, will be called the standard local-mode representation.

By analogy to the equations (2.4) and (2.5), the first term $\varphi_0(x)Z_0(z;x)$ of the series (4.4) will be called the propagating mode, while the remaining terms $\varphi_n(x)Z_n(z;x)$, $n = 1, 2, \ldots$, will be called the evanescent modes (or non-propagating modes). The function $Z_n(z;x)$ represents the vertical structure of the nth mode. The function $\varphi_n(x)$ describes the horizontal pattern of the nth mode and will be called the complex amplitude of the nth mode.

Property (4.3b) of the local vertical eigenfunctions implies that the wave potential $\varphi^{(2)}(x,z)$, as defined by equation (4.4), satisfies identically the free-surface boundary condition, equation (2.8b). Consequently, the use of the standard representation renders the free-surface boundary condition an essential condition in relation to the variational formulation presented in the previous section. On the other hand, the function $\varphi^{(2)}(x,z)$, as defined through (4.4), is incompatible with bottom boundary condition of the problem if $\mathrm{d}h(x)/\mathrm{d}x \neq 0$. For, by differentiating (4.4) with respect to z and using property (4.3c) of the local vertical eigenfunctions, we obtain

$$[\partial\varphi^{(2)}(x,z)/\partial z]_{z=-h(x)} = 0 \quad (a < x < b), \tag{4.5}$$

which is in contradiction to (2.8c) in the case of a sloping bottom. This contradiction also affects the conservation of energy. In the absence of any energy dissipation mechanism, the average wave power $P(x)$, transmitted through any vertical section

extending from the bottom $z = -h(x)$ up to the mean water level $z = 0$, must be constant; that is $\mathrm{d}P(x)/\mathrm{d}x = 0$. The quantity $\mathrm{d}P(x)/\mathrm{d}x = 0$ can be expressed analytically in terms of the wave potential $\varphi(x, z)$, in the form

$$\frac{\mathrm{d}P(x)}{\mathrm{d}x} = \frac{\rho g^2 H^2}{8\omega} \mathrm{Im} \left\{ \left[\frac{\mathrm{d}h}{\mathrm{d}x} \varphi^* \frac{\partial \varphi}{\partial x} + \varphi^* \frac{\partial \varphi}{\partial z} \right]_{z=-h(x)} \right\}, \tag{4.6}$$

where H is the incident wave height. By substituting the potential $\varphi^{(2)}$ from (4.4) into (4.6), we observe that $\mathrm{d}P/\mathrm{d}x$ will be necessarily non-zero in any variable bathymetry position, since, in this case, $\partial\varphi^{(2)}/\partial z = 0$, while $\mathrm{d}h/\mathrm{d}x \neq 0$ and $\varphi^{(2)^*}(\partial\varphi^{(2)}/\partial x) \neq 0$. Only in the case of a mild-slope bottom, i.e. when $|\mathrm{d}h/\mathrm{d}x|/(k_0 h) \ll 1$, is the discrepancy expected to be small and, thus, the representation (4.4) can be considered approximately valid. This deficiency of the standard local-mode representation has also been discussed (but not resolved) by Rutherford & Hawker (1981) in the context of hydroacoustic applications. The removal of this drawback of the standard local-mode representation of the wave potential is the main goal of the present paper.

The drawback of the representation (4.4) in the case of a sloping bottom lies in the fact that the infinite series appearing in the right-hand side does not converge uniformly in the interval $[-h(x), 0]$. We recall here that the series expansion in terms of $Z_n(z; x)$, $n = 0, 1, 2, \ldots$, of any C^2-function $f(z)$ is uniformly convergent in $[-h(x), 0]$ only if $f(z)$ satisfies both boundary conditions (4.3*b*, *c*); see, e.g. Coddington & Levinson (1955 ch. 7.4). Otherwise, if $f(z)$ does not satisfy the boundary condition (4.3*b* or *c*), the convergence is uniform only in subintervals of the form $[-h(x)+\varepsilon, -\varepsilon]$, and the limit of the series at $z = 0$ or $z = -h(x)$ may not coincide with the end value(s) of $f(z)$. Thus, representation (4.4) is inappropriate to treat the boundary-value problem $\mathscr{P}_T(D^{(2)}, \mu, A_0)$, which imposes a boundary condition at $z = -h(x)$, incompatible with the boundary behaviour of the basis functions. One way to overcome this problem is to modify the function which is to be expanded, ensuring that the modified function satisfies exactly the same boundary conditions as $Z_n(z; x)$ at both endpoints $z = 0$ and $z = -h(x)$.

4.2. *Enhancement of the representation by means of an additional mode*

In this subsection, we shall describe how to modify the expansion (4.4), in order to ensure that the series (4.4) converges uniformly in the closed interval $[-h(x), 0]$. The basic idea is to subtract an appropriate function $\varphi^{(2)}_{-1}(x, z)$ from the wave potential $\varphi^{(2)}(x, z)$, so that the difference

$$f^{(2)}(x, z) = \varphi^{(2)}(x, z) - \varphi^{(2)}_{-1}(x, z) \tag{4.7}$$

satisfies the boundary conditions

$$\frac{\partial f^{(2)}(x, z)}{\partial z} - \mu f^{(2)}(x, z) = 0 \quad (z = 0) \tag{4.8a}$$

$$\frac{\partial f^{(2)}(x, z)}{\partial z} = 0 \quad (z = -h(x)), \tag{4.8b}$$

for every $x \in [a, b]$. Boundary conditions (4.8*a*, *b*) are exactly the same as the boundary conditions (4.3*b*, *c*), satisfied by the basis functions $Z_n(z; x)$, $n = 0, 1, 2, \ldots$. Thus, the expansion of the function $f^{(2)}(x, z)$ in terms of $Z_n(z; x)$, $n = 0, 1, 2, \ldots$,

$$f^{(2)}(x, z) \equiv \varphi^{(2)}(x, z) - \varphi^{(2)}_{-1}(x, z) = \varphi_0(x) Z_0(z; x) + \sum_{n=1}^{\infty} \varphi_n(x) Z_n(z; x), \tag{4.9}$$

converges uniformly in $[-h(x), 0]$. The coefficients $\varphi_n(x)$ appearing in (4.9) are, of course, different from the corresponding coefficients appearing in (4.4).

To proceed further we have to construct an appropriate representation for the function $\varphi_{-1}^{(2)}(x, z)$. A possible choice is

$$\varphi_{-1}^{(2)}(x, z) = \varphi_{-1}(x) Z_{-1}(z; x), \tag{4.10}$$

where $Z_{-1}(z; x)$ is any smooth z-function in $[-h(x), 0]$ satisfying the conditions

$$\frac{\partial Z_{-1}(z = 0, x)}{\partial z} - \mu Z_{-1}(z = 0, x) = 0, \quad \frac{\partial Z_{-1}(z = -h(x), x)}{\partial z} = 1, \tag{4.11a, b}$$

for each $x \in [a, b]$. We remark that condition (4.11*a*) implies that both $\varphi_{-1}^{(2)}(x, z)$ and $f^{(2)}(x, z)$ satisfy the free-surface condition, and condition (4.11*b*), in conjunction with equations (4.10) and (4.9), implies that

$$\varphi_{-1}(x) = [\partial \varphi^{(2)} / \partial z]_{z=-h(x)}. \tag{4.12}$$

Recalling that all terms in the standard local-mode expansion have zero vertical derivative on the bottom ($z = -h(x)$), we can interpret $\varphi_{-1}(x)$ as a set of additional degrees of freedom, accounting for the non-homogeneity in the vertical derivative caused by a sloping bottom.

A specific convenient form of the function $Z_{-1}(z; x)$ is given by

$$Z_{-1}(z; x) = h(x) \left[\left(\frac{z}{h(x)} \right)^3 + \left(\frac{z}{h(x)} \right)^2 \right]. \tag{4.13a}$$

Numerical results presented in this work are based on this choice for $Z_{-1}(z; x)$. However, other choices are also possible, as, for example, the function:

$$Z_{-1}(z; x) = -\frac{z^2}{2h(x)} \cosh [K(z + h(x))], \tag{4.13b}$$

where K is a constant.

Equation (4.12) is a necessary and sufficient condition in order that $f^{(2)}(x, z)$ satisfies (4.8*b*), under the conditions (4.10) and (4.11). However, (4.12) cannot be used for the calculation of $\varphi_{-1}(x)$, since the value of $\partial \varphi^{(2)} / \partial z$ at $z = -h(x)$ is not known *a priori*. In fact, (4.12) provides us with an additional amplitude function, which will be coupled with all other amplitude functions $\varphi_n(x), n = 0, 1, \ldots$, by means of the variational equation (3.3*b*). See § 5.

In conclusion, we have arrived at the following representation of the wave potential in $D^{(2)}$:

$$\varphi^{(2)}(x, z) = \varphi_{-1}(x) Z_{-1}(z; x) + \varphi_0(x) Z_0(z; x) + \sum_{n=1}^{\infty} \varphi_n(x) Z_n(z; x) = \sum_{n=-1}^{\infty} \varphi_n(x) Z_n(z; x), \tag{4.14}$$

which, in comparison with (4.4), contains the additional term $\varphi_{-1}(x) Z_{-1}(z; x)$. This is exactly the correction term required in order to make possible the satisfaction of the bottom boundary condition, equation (2.8*c*). This term will be subsequently called the sloping-bottom mode, and the representation (4.14) will be referred to as the enhanced local-mode representation.

We are now in a position to give the definition of an admissible function space $\boldsymbol{A}(D^{(2)})$ for the function $\varphi^{(2)}(x, z)$, to be used in conjunction with the variational

principle of the problem $\mathscr{P}_T(D^{(2)}, \mu, A_0)$, stated in theorem 1. This function space is defined by

$$\boldsymbol{A}(D^{(2)}) = \{\psi(x,z) \in \boldsymbol{C}^2(D^{(2)}) \cap \boldsymbol{C}^1(\overline{D}^{(2)}) \colon\ \partial\psi/\partial z - \mu\psi = 0 \text{ on } \partial D_F^{(2)}\}, \tag{4.15}$$

where $\boldsymbol{C}^k(\circ)$ are the usual spaces of functions having continuous derivatives up to order k, and $\overline{D}^{(2)} = D^{(2)} \cup \partial D^{(2)}$. It is more restricted than the one assumed in formulating theorem 1, since all of its elements satisfy *a priori* the free-surface condition. This more efficient choice for the admissible functions $\varphi^{(2)}(x,z)$ is accurately restated in the form of theorem 2.

THEOREM 2 [*The representation theorem*]. *Any function* $\psi(x,z) \in \boldsymbol{A}(D^{(2)})$ *can be uniquely expanded in a series of the form*

$$\psi(x,z) = \sum_{n=-1}^{\infty} \psi_n(x) Z_n(z;x) \quad (a \leqslant x \leqslant b, \quad -h(x) \leqslant z \leqslant 0), \tag{4.16}$$

where $Z_n(z;x)$ *are given by* (4.2) *and* (4.13), *for* $n = 0, 1, 2, \ldots$, *and* $n = -1$, *respectively, and* $\psi_n(x)$ *are appropriate amplitude functions belonging to* $C^2((a,b)) \cap C^1([a,b])$. *Representation* (4.16) *is absolutely and uniformly, along with its termwise derivatives, convergent in the closed domain* $D^{(2)} = \{(x,z), \quad a \leqslant x \leqslant b, \quad -h(x) \leqslant z \leqslant 0\}$.

It is important to realize here that, the arbitrariness of the choice of the function $Z_{-1}(z;x)$ renders the coefficients $\psi_n(x)$ dependent on the specific choice. This is equivalent to a change of the basis of $\boldsymbol{A}(D^{(2)})$, which does not affect the validity of the expansion (4.16).

5. Coupled-mode system of equations

Let us reconsider the variational principle, theorem 1, assuming that $\varphi^{(2)}(x,z) \in A(D^{(2)})$. Then, by means of the enhanced representation (4.14) (see also theorem 2), the functional $\mathscr{F}(\varphi^{(2)}, A_R, \{C_n^{(1)}\}_{n\in N}, A_T, \{C_n^{(3)}\}_{n\in N})$, given by equation (3.1), is transformed to an equivalent functional of the form

$$\mathscr{F} = \mathscr{F}\left(\begin{matrix} b \\ \varphi_{-1}(x), \\ a \end{matrix} \left\{ \begin{matrix} b \\ \varphi_n(x) \\ a \end{matrix} \right\}_{n=0,1,2,\ldots}, \quad A_R, \{C_n^{(1)}\}_{n\in N}, \quad A_r, \{C_n^{(3)}\}_{n\in N} \right), \tag{5.1}$$

where a and b denote the range of the dummy variable x, according to Volterra's notation, Volterra (1929). In this way, the degrees of freedom of the system associated with the admissible wave potential $\varphi^{(2)}(x,z)$ in $D^{(2)}$ (interior points) and $\varphi^{(2)}(x,z)$ on $\partial D_{\Pi}^{(2)}$ (bottom boundary values) are equivalently described by the modal amplitudes $\varphi_n(x), x \in (a,b), n = -1, 0, 1, \ldots$. Associated with the vertical interfaces $\partial D_I^{(12)}$ and $\partial D_I^{(23)}$ are the degrees of freedom $\{\varphi_n(a)\}_{n=0,1,\ldots}$ and $\{\varphi_n(b)\}_{n=0,1,\ldots}$ of the amplitude values at the left-endpoint $x = a$, and at the right-endpoint $x = b$, respectively, as well as the sets of coefficients $\{A_R, C_n^{(1)}, n = 0, 1, 2, \ldots\}$ and $\{A_T, C_n^{(3)}, n = 0, 1, 2, \ldots\}$. Especially, for the sloping-bottom amplitude $\varphi_{-1}(x)$, the following end conditions are imposed:

$$\varphi_{-1}(a) = \varphi_{-1}(b) = 0, \quad \varphi'_{-1}(a) = \varphi'_{-1}(b) = 0, \tag{5.2}$$

in accordance with equation (4.12) and the smoothness assumptions concerning the depth function $h(x)$.

The use of a different (equivalent) set of degrees of freedom of the system in the variational principle leads to a different (equivalent) set of equations for the same problem $\mathscr{P}_T(D^{(2)}, \mu, A_0)$. This point will be exploited in the next subsection.

5.1. *Horizontal coupled-mode system of equations*

Taking into account that any admissible function $\varphi^{(2)}$ satisfies the free-surface boundary condition, equation (2.8*b*), the third integral in the left-hand side of (3.3*b*) can be dropped. Moreover, by assuming that all variations except $\delta\varphi^{(2)}(x,z)$ in $D^{(2)} \cup \partial D_{II}^{(2)}$ are kept zero, the last four integrals of (3.3*b*) can be dropped, and thus we obtain

$$-\int_{D(2)} (\nabla^2\varphi^{(2)})\delta\varphi^{(2)}\mathrm{d}V + \int_{\partial D_{II}^{(2)}} \left(\frac{\partial\varphi^{(2)}}{\partial n^{(2)}}\right)\delta\varphi^{(2)}\mathrm{d}S = 0. \tag{5.3}$$

By introducing in the above equation the representation (4.14) for $\varphi^{(2)}$, and its consequence concerning the expression of $\delta\varphi^{(2)}$, and by using the geometrical relation

$$\left(n_x^{(2)}, n_z^{(2)}\right) = -(h'(x), 1)/\sqrt{1 + (h'(x))^2} \quad ((x,z) \in \partial D_{II}^{(2)}), \tag{5.4}$$

we obtain the variational equation:

$$\sum_{m=-1}^{\infty} \int_{x=a}^{x=b} \delta\varphi_m(x) \left[\sum_{n=-1}^{\infty} a_{mn}(x)\varphi_n''(x) + b_{mn}(x)\varphi_n'(x) + c_{mn}(x)\varphi_n(x)\right] \mathrm{d}x = 0, \tag{5.5}$$

where a prime denotes differentiation with respect to x. The x-dependent coefficients $a_{mn}(x)$, $b_{mn}(x)$ and $c_{mn}(x)$ are given in table 1. Since $\delta\varphi_m(x), m = -1, 0, 1, \ldots$ are arbitrary, independent variations, equation (5.5) is equivalent to the following infinite system

$$\sum_{n=-1}^{\infty} a_{mn}(x)\varphi_n''(x) + b_{mn}(x)\varphi_n'(x) + c_{mn}(x)\varphi_n(x) = 0 \quad (a < x < b, \quad m = -1, 0, 1, \ldots), \tag{5.6}$$

which will be called the coupled-mode system of horizontal equations. From the above derivation it is clear that the system (5.6) is related to both the Laplace equation (field equation) and the bottom boundary condition, and it is the additional sloping-bottom mode that permits the simultaneous satisfaction of both equations.

Before proceeding further, let us consider two special cases included in (5.6). In the case when the sloping-bottom mode is neglected, the extended mild-slope equation (system of equations), derived by Massel (1993) and Porter & Staziker (1995), is obtained. If in addition all evanescent modes are omitted, and the representation is left only with the propagating mode ($n = 0$), equation (5.6) reduces to the modified mild-slope equation derived by Massel (1993) and Chamberlain & Porter (1995).

5.2. *Boundary conditions for the modal amplitude functions*

Since the system (5.6) is equivalent to (5.3), retaining the former renders the latter an identity. Thus, the variational equation (3.3*b*) can now be simplified to:

$$\begin{aligned}\int_{\partial D_I^{(12)}} \left(\frac{\partial\varphi^{(2)}}{\partial n^{(2)}} + \frac{\partial\varphi^{(1)}}{\partial n^{(1)}}\right)\delta\varphi^{(2)}\mathrm{d}S + \int_{\partial D_I^{(23)}} \left(\frac{\partial\varphi^{(2)}}{\partial n^{(2)}} + \frac{\partial\varphi^{(3)}}{\partial n^{(3)}}\right)\delta\varphi^{(2)}\mathrm{d}S \\ + \int_{\partial D_I^{(12)}} (\varphi^{(2)} - \varphi^{(1)})\delta\left(\frac{\partial\varphi^{(1)}}{\partial x}\right)\mathrm{d}S - \int_{\partial D_I^{(23)}} (\varphi^{(2)} - \varphi^{(3)})\delta\left(\frac{\partial\varphi^{(3)}}{\partial x}\right)\mathrm{d}S = 0.\end{aligned} \tag{5.7}$$

	$m=-1$ $n=-1,0,1,2,\ldots$	$m=0,1,2,\ldots$ $n=-1$	$m=0,1,2,\ldots$ $n=0,1,2,\ldots$
$a_{mn}(x)$	$\langle Z_{-1}, Z_n\rangle$	$\langle Z_m, Z_{-1}\rangle$	$\delta_{nm}\|Z_m\|^2$
$b_{mn}(x)$	$2\langle Z_{-1}, \partial Z_n/\partial x\rangle$	$2\langle Z_m, \partial Z_{-1}/\partial x\rangle$	$2\langle Z_m, \partial Z_n/\partial x\rangle$ $+h'(x)Z_m(-h)\,Z_n(-h)$
$c_{mn}(x)$	$\langle Z_{-1}, \Delta Z_n\rangle$	$\langle Z_m, \Delta Z_{-1}\rangle$ $+\left(1+h'(x)\dfrac{\partial Z_{-1}(-h)}{\partial x}\right)$ $\times Z_m(-h)$	$\langle Z_m, \Delta Z_n\rangle$ $+h'(x)Z_m(-h)$ $\times(\partial Z_n(-h)/\partial x)$

Where $Z_n = Z_n(z;x)$ is parametrically dependent on x through $h(x)$

$$\Delta = \frac{\partial^2}{\partial z^2} + \frac{\partial^2}{\partial x^2}, \quad \langle f, g\rangle = \int_{-h(x)}^{0} f(z)g(z)\mathrm{d}z, \quad \|f\|^2 = \langle f, f\rangle$$

$$\text{For } n=0,1,\ldots \quad \Delta Z_n = \frac{\partial^2 Z_n}{\partial x^2} - (k_n)^2 Z_n$$

TABLE 1. Coefficients of the coupled-mode system, equation (5.6).

By assuming that all variations in (5.7), except $\delta\varphi^{(2)}$ on $\partial D_I^{(12)}$, are kept zero, we obtain the equation

$$\int_{\partial D_I^{(12)}} \left(\frac{\partial\varphi^{(2)}}{\partial n^{(2)}} + \frac{\partial\varphi^{(1)}}{\partial n^{(1)}}\right)\delta\varphi^{(2)}\mathrm{d}S = 0. \tag{5.8}$$

Expressing the normal derivative $\partial\varphi^{(1)}/\partial n^{(1)}$ of the wave potential on the left-matching boundary $\partial D_I^{(12)}$ by means of the termwise differentiated series (2.4), and using equations (4.14) and (5.2), equation (5.8) takes the form:

$$\sum_{m=0}^{\infty}\delta\varphi_m(a)\int_{z=-h_1}^{0}\left\{\left((\mathrm{i}k_0^{(1)}A_0\exp(\mathrm{i}k_0^{(1)}a) - \mathrm{i}k_0^{(1)}A_R\exp(-\mathrm{i}k_0^{(1)}a))Z_0^{(1)}(z)\right.\right.$$
$$\left.\left.-\varphi_0'(a)Z_0(z;a)\right) + \sum_{n=1}^{\infty}(k_n^{(1)}C_n^{(1)}Z_n^{(1)}(z) - \varphi_n'(a)Z_n(z;a))\right\}Z_m(z;a)\mathrm{d}z = 0. \tag{5.9}$$

As $x\to a+0$, then $h(x)\to h_1$ in C^2-sense, and, thus, the local basis $\{Z_n(z;x)\}_{n=0,1,\ldots}$ converges to the left-strip basis $\{Z_n^{(1)}(z)\}_{n=0,1,\ldots}$, uniformly for $z\in[h_1,0]$. Exploiting this property, in conjunction with the orthogonality of the functions $Z_n^{(1)}(z), n=0,1,2\ldots$, and the arbitrariness of the variations $\delta\varphi_n(a)$, we obtain from (5.9) the following set of conditions at $x=a$:

$$\varphi'_0(a) = \mathrm{i}k_0^{(1)}(A_0\exp(\mathrm{i}k_0^{(1)}a) - A_R\exp(-\mathrm{i}k_0^{(1)}a)), \quad \varphi_n'(a) = k_n^{(1)}C_n^{(1)} \quad (n=1,2,\ldots). \tag{5.10a,b}$$

We now continue by considering that all variations in (5.7), except $\delta(\partial\varphi^{(1)}/\partial x)$ on $\partial D_I^{(12)}$, are kept zero. On this basis, we obtain

$$\int_{\partial D_I^{(12)}}(\varphi^{(2)}-\varphi^{(1)})\,\delta\left(\frac{\partial\varphi^{(1)}}{\partial x}\right)\mathrm{d}S = 0. \tag{5.11}$$

By substituting equations (4.14) and (2.4) into equation (5.11), and using equation (5.2), we obtain the equation:

$$\int_{z=-h_1}^{0} \left\{ \left(\left(A_0 \exp(\mathrm{i}k_0^{(1)}a) + A_R \exp(-\mathrm{i}k_0^{(1)}a) \right) Z_0^{(1)}(z) - \varphi_0(a) Z_0(z;a) \right) + \sum_{n=1}^{\infty} \left(C_n^{(1)} Z_n^{(1)}(z) - \varphi_n(a) Z_n(z;a) \right) \right\} \times \left\{ -\mathrm{i}k_0^{(1)} \exp(-\mathrm{i}k_0^{(1)}a) Z_0^{(1)}(z) \delta A_R + \sum_{m=1}^{\infty} k_m^{(1)} Z_m^{(1)}(z) \delta C_m^{(1)} \right\} \mathrm{d}z = 0. \tag{5.12}$$

Using the same arguments as above, we obtain from equation (5.12) the following set of conditions at $x = a$:

$$\varphi_0(a) = A_0 \exp(\mathrm{i}k_0^{(1)}a) + A_R \exp(-\mathrm{i}k_0^{(1)}a), \quad \varphi_n(a) = C_n^{(1)} \quad (n = 1, 2, \ldots). \tag{5.13a, b}$$

Working similarly with the terms of equation (5.7) defined on the right-matching boundary $\partial D_I^{(23)}$, we derive the following set of conditions at $x = b$:

$$\varphi_0(b) = A_T \exp(\mathrm{i}k_0^{(3)}b), \quad \varphi_n(b) = C_n^{(3)} \quad (n = 1, 2, \ldots), \tag{5.14a, b}$$

$$\varphi_0'(b) = \mathrm{i}k_0^{(3)} A_T \exp(\mathrm{i}k_0^{(3)}b), \quad \varphi_n'(b) = -k_n^{(3)} C_n^{(3)} \quad (n = 1, 2, \ldots). \tag{5.15a, b}$$

Clearly, the unknown coefficients $A_R, C_n^{(1)}, n = 1, 2, \ldots$ ($A_T, C_n^{(3)}, n = 1, 2, \ldots$) can be eliminated from (5.10), (5.13) (Eqs. (5.14), (5.15)), obtaining Robin conditions for φ_0 and $\varphi_n, n = 1, 2 \ldots$ at $x = a$ ($x = b$). Recapitulating the above results we can state the following theorem.

THEOREM 3 [*The coupled-mode system*]. *The variational equation* (3.3) *and, thus, the transmission problem* $\mathscr{P}_T(D^{(2)}, \mu, A_0)$, *are equivalent to the following system of second-order differential equations*:

$$\sum_{n=-1}^{\infty} a_{mn}(x)\varphi_n''(x) + b_{mn}(x)\varphi_n'(x) + c_{mn}(x)\varphi_n(x) = 0 \quad (a < x < b, \quad m = -1, 0, 1, \ldots). \tag{5.16}$$

in $a < x < b$, *supplemented by the boundary conditions*

$$\varphi_{-1}(a) = \varphi_{-1}'(a) = 0, \quad \varphi_{-1}(b) = \varphi_{-1}'(b) = 0, \tag{5.17a, a'}$$

$$\varphi_0'(a) + \mathrm{i}k_0^{(1)}\varphi_0(a) = 2\mathrm{i}k_0^{(1)} A_0 \exp(\mathrm{i}k_0^{(1)}a), \quad \varphi_n'(a) - k_n^{(1)}\varphi_n(a) = 0 \quad (n = 1, 2, \ldots), \tag{5.17b, b'}$$

$$\varphi_0'(b) - \mathrm{i}k_0^{(3)}\varphi_0(b) = 0, \quad \varphi_n'(b) + k_n^{(3)}\varphi_n(b) = 0 \quad (n = 1, 2, 3, \ldots). \tag{5.17c, c'}$$

The coefficients $A_R, C_n^{(1)}, A_T, C_n^{(3)}$ *are then obtained by the equations*:

$$A_R = (\varphi_0(a) - A_0 \exp(\mathrm{i}k_0^{(1)}a)) \exp(\mathrm{i}k_0^{(1)}a), \quad C_n^{(1)} = \varphi_n(a) \quad (n = 1, 2, 3, \ldots) \tag{5.18a, a'}$$

$$A_T = \varphi_0(b) \exp(-\mathrm{i}k_0^{(3)}b), \quad C_n^{(3)} = \varphi_n(b) \quad (n = 1, 2, 3, \ldots). \tag{5.18b, b'}$$

Remarks. (i) The forcing of the system, due to the incident wave, appears only in the boundary condition (5.17*b*). (ii) Under the smoothness assumptions for the depth function $h(x)$, all coefficients $a_{mn}(x), b_{mn}(x), c_{mn}(x)$ of the system are continuous functions of x and can be calculated by means of the solution of the local (vertical) eigenvalue problem. (iii) Discontinuities of $h(x)$ or $h'(x)$ can also be treated by introducing appropriate domain decomposition with matching boundaries at the points of discontinuities; cf. Porter & Chamberlain (1997). (iv) The present theory can be straightforwardly extended to treat the case where waves are incident from both directions ($\pm\infty$) simultaneously, as well as the case of obliquely incident waves.

The theoretical investigation of the coupled-mode system, i.e. the appropriate function space setting, uniqueness and existence results and other properties of the solution, seems to be very challenging. Nevertheless, in the sequel of the present work we shall focus on a detailed numerical investigation of the coupled-mode system (5.16), (5.17), which also provides the ground for stating some interesting and very useful theoretical conjectures.

6. Numerical results and discussion

In this section, a discrete scheme for the numerical solution of the enhanced coupled-mode system, equations (5.16), (5.17), is introduced, and extensive numerical results concerning the problem $\mathscr{P}_T(D, \mu, A_0)$ for various values of the involved parameters are presented. Also, comparative calculations obtained by using the present method (enhanced local-mode representation), the extended mild-slope (standard local-mode representation, Massel 1993; Porter & Staziker 1995), as well as the modified mild-slope equation (Massel 1993; Chamberlain & Porter 1995) are presented and discussed.

6.1. *Discrete approximation of the coupled-mode system of equations*

All numerical results presented in this section are based on the choice (4.13*a*) for $Z_{-1}(z; x)$. However, extensive numerical experimentation with other possible choices, such as the form (4.13*b*) and others, have proved that the final result concerning the wave potential as obtained by the enhanced representation (4.14) is exactly the same for all valid forms of $Z_{-1}(z; x)$.

Truncating the series (4.14) to a finite number of terms (modes), and denoting by N_e the number of evanescent modes retained, the following approximation of the wave potential in $D^{(2)}$ is obtained

$$\varphi^{(2)}(x, z) = \sum_{n=-1}^{N_e} \varphi_n(x) Z_n(z; x). \tag{6.1}$$

The construction of the discrete system is completed by using central, second-order finite differences to approximate the derivatives in the coupled mode system (5.16). Discrete boundary conditions are obtained by combining equations (5.16) and (5.17) and then using central differences to approximate derivatives. Thus, the discrete scheme obtained in this way is uniformly of second order in the horizontal direction. On the basis of the above considerations, the coupled-mode system of differential equations (5.16), (5.17) is finally reduced to a linear algebraic system. The coefficient matrix of the system is banded three-diagonal and has a dimension $N_d = (N_e + 2)(N + 1)$, where N is the number of segments subdividing the interval $[a, b]$. The forcing appears only in one equation ($n = 0$), at the left endpoint $x = a$ (see (5.17*b*)).

As concerns the condition of the discrete coefficient matrix, although its condition

number increases with N_e, still, in all numerical cases examined, it is found to remain several orders of magnitude below the limit imposed by the computer's precision. On the other hand, a minimum number of 20–30 points per horizontal wavelength is found to be sufficient to obtain accurate results.

6.2. *Presentation of numerical results and discussion*

Before proceeding to a detailed presentation of the numerical results obtained, we introduce some terminology. The abbreviations ER, SR and MMS are used to denote results obtained by using the enhanced representation (present method), the standard representation (i.e. the extended mild-slope equation), and the modified mild-slope equation, respectively. Also, the same codes, ER, SR, MMS, will be used as prefixes in order to distinguish physical quantities calculated with the aid of corresponding methods (e.g. ER-amplitudes etc.).

6.2.1. *The case of a smooth underwater shoaling*

This topography has been considered by Massel (1993) in order to demonstrate the effects of bottom slope and curvature on the solution obtained by his modified mild-slope equation. The environment is characterized by the following depth function

$$h(x) = h_m(x) = \begin{cases} h_1 = 6\,\mathrm{m} & (x < a = 0) \\ \frac{1}{2}(h_1 + h_3) - \frac{1}{2}(h_1 - h_3)\tanh\left(3\pi\left(\dfrac{x}{b} - \dfrac{1}{2}\right)\right) & (a < x < b) \\ h_3 = 2\,\mathrm{m} & (x > b = 20\,\mathrm{m}), \end{cases} \tag{6.2}$$

which models a smooth but steep underwater shoaling, with maximum slope $s_{max} = 0.94$ and mean slope $s_{mean} = 0.2$. (A sketch of the bottom geometry is shown in figure 4.) The angular frequency of the incident wave is taken to be $\omega = 2\,\mathrm{rad/sec}$, implying that both ratios $h_1/\lambda_1 = 0.4$ and $h_3/\lambda_3 = 0.17$ fall well outside the limits of the deep or the shallow water theory.

In figure 2 the moduli of the modal-amplitude functions, i.e. the quantities $|\varphi_n(x)|$, $a \leqslant x \leqslant b$, are presented, as obtained by using both the ER and the SR. The horizontal axis in figure 2 is a multiple replica of the interval $[a, b]$, i.e. a sequence of repeated intervals $[a, b]$, each one associated with a mode, and named after the mode number. In the nth replica of interval $[a, b]$ the amplitude $|\varphi_n(x)|$ of the nth mode is plotted. For example, in the interval indicated by the number 7, the function $|\varphi_7(x)|$ is plotted *vs.* $x \in [a, b]$, as obtained by the ER and SR, respectively. Numerical results shown have been obtained by subdividing the range $b - a = 20\,\mathrm{m}$ into $N = 100$ segments and retaining $N_e = 13$ modes in ER and $N_e = 14$ modes in SR, respectively. This choice was made in order to keep the same dimension of the discrete system in the two cases ($N_d = 1515$). Also, in the same figure, the curves $0.1\,n^{-4}$ and $0.1\,n^{-2}$ are drawn, which bound the maxima of the amplitudes of the modal functions as obtained by the ER and the SR, respectively. Thus, assuming that these bounding curves remain valid for all n, we can conjecture that the ER-amplitudes decay as $O(n^{-4})$, while the SR-amplitudes decay as $O(n^{-2})$. (Numerical evidence completely supports this conjecture; a rigorous mathematical proof is also highly desirable.) Note that the rate of decay $O(n^{-2})$ of the SR-amplitudes is not sufficient to ensure the uniform convergence (up to the bottom) of the series representing the velocity field, which thus may converge only in the L^2-sense. This problem is remedied by means of the ER-solution, since the rate of decay of ER-amplitudes is $O(n^{-4})$, which ensures the absolute and uniform convergence up to (and including) the boundaries.

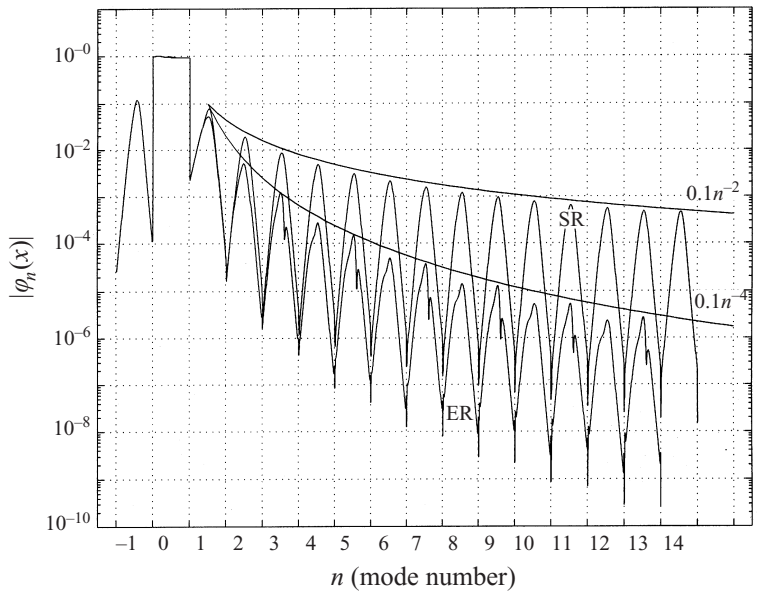

FIGURE 2. Moduli $|\varphi_n(x)|$ of the modal-amplitude functions *vs.* $x \in [a, b]$, for various modes $n = -1, 0, 1, \ldots, 14$. The depth function is given by equation (6.2). Wave frequency $\omega = 2\,\mathrm{rad\,s^{-1}}$. The curves $0.1\,n^{-4}$ and $0.1\,n^{-2}$ bound the maxima of the amplitudes of the modal functions as obtained by the ER and the SR, respectively.

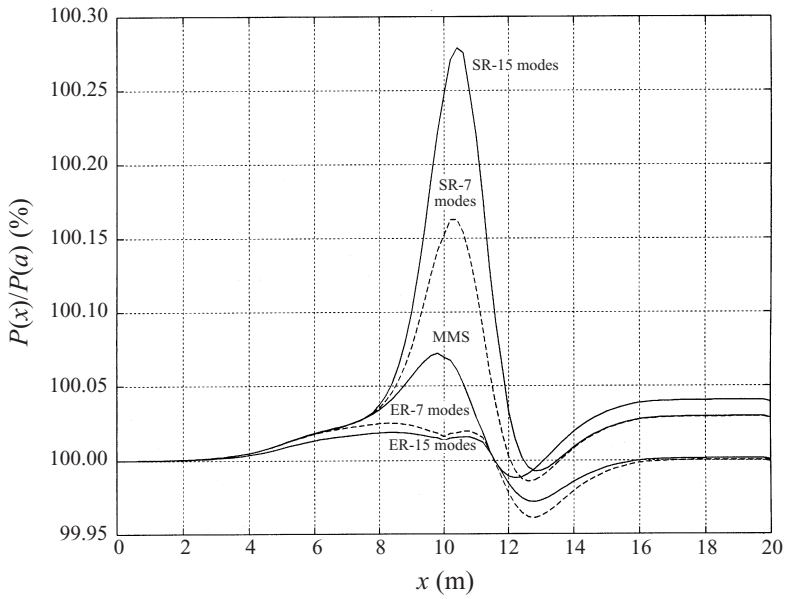

FIGURE 3. Variation of the wave power flux $P(x)$ through a vertical section at x *vs.* $x \in [a, b]$. The depth function is given by equation (6.2). Wave frequency $\omega = 2\,\mathrm{rad\,s^{-1}}$.

In figure 3 the variation of the wave power flux $P(x)$ through a vertical section in the variable bathymetry region is presented. The level 100% in the vertical axis corresponds to the level of power flux entering the domain at $x = a$, that should remain constant for all x. The numerical results presented are obtained by using the ER, SR

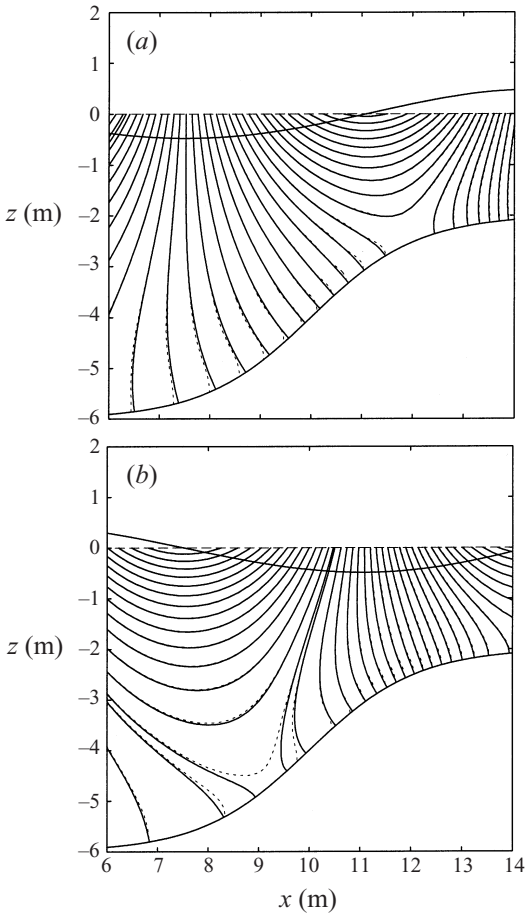

FIGURE 4. Equipotential lines of the wave field and free-surface elevation in the variable bathymetry region, as obtained by ——, the ER model and – – –, the SR model, respectively. The depth function is given by equation (6.2). The angular frequency of the incident wave is $\omega = 2\,\mathrm{rad\,s^{-1}}$ and its height $H = 1\,\mathrm{m}$. (*a*) Real parts of the wave potential $\Phi(x,z) = -0.5(\mathrm{i}gH/\omega)\varphi(x,z)$ and the free-surface elevation $\zeta(x) = 0.5H\varphi(x,z=0)$. (*b*) Imaginary parts of the wave potential and the free-surface elevation.

and the MMS models. The results obtained by using the ER and the MMS models are fairly compatible with the conservation of energy (cf. the discussion in § 4). On the contrary, the SR results exhibit a larger deviation from the conservation of energy and, most importantly, this deviation becomes larger as the number of evanescent modes increases. This surprising effect is a manifestation of the incompatibility of the standard representation with the sloping-bottom boundary condition; see equation (4.6).

In figure 4 the equipotential lines of the wave field (real and imaginary part) in the variable bathymetry subdomain $D^{(2)}$ have been plotted, together with the calculated free-surface elevation, as obtained by the ER model (solid lines) and the SR model (dotted lines), respectively. The height of the incident wave is $H = 1\,\mathrm{m}$. This figure is obtained by retaining 6 evanescent modes ($N_e = 6$) in the representation, which is enough for numerical convergence. The pattern shown by the solid lines in figure 4 is quite reasonable and the equipotential lines intersect the bottom profile

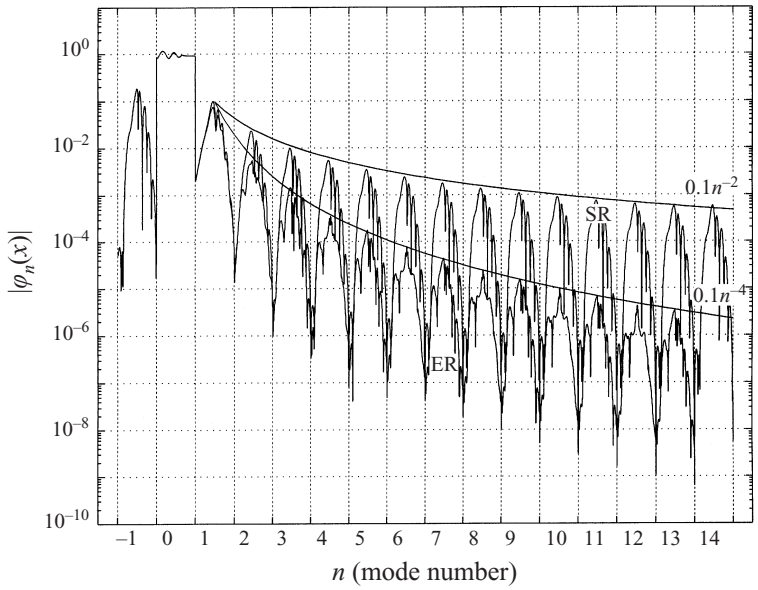

FIGURE 5. The same as figure 2, but for the depth function given by equation (6.3).

perpendicularly, as they ought. This result justifies the concept of the sloping-bottom mode, which constitutes the main contribution of the present work. The fact that the SR solution satisfies the condition $\partial\varphi^{(2)}/\partial z = 0$ at the bottom is clearly seen in this figure; SR-lines bend and become vertical near the bottom, independently of the bottom slope. This erroneous estimation of the velocity near and on the bottom surface is also responsible for the violation of the conservation of energy. Compare this with the discussion of figure 3.

6.2.2. *The case of an underwater shoaling with bottom corrugations*

For a deeper understanding of the numerical behaviour of the ER model, another, more complicated, environment was also studied. This environment is characterized by the depth function

$$h(x) = h_m(x) + h_c(x) = h_m(x) + 0.67\exp\left(-0.05(x-12.5)^2\right)\cos\left(x-12.5\right)\mathrm{m}, \qquad (6.3)$$

where the mean depth $h_m(x)$ is the smooth shoaling defined by equation (6.2), and $h_c(x)$ is a perturbation giving rise to bottom corrugations that gradually vanish at the ends of the variable bathymetry subdomain. (A sketch of the bottom geometry is shown in figure 7). The angular frequency of the incident wave is taken, as before, to be $\omega = 2\,\mathrm{rad\,s^{-1}}$, and the ratio of the wavelength of bottom corrugations to the wavelength of the incident wave is $\Lambda/\lambda_1 \approx 0.42$. The local bottom slope attains its maximum value $s_{max} \approx 1.2$ approximately at the middle of the variable bathymetry region.

In figure 5 the moduli $|\varphi_n(x)|$ of the modal-amplitude functions are comparatively presented as obtained by the ER and the SR models, respectively. Compare this with the discussion of figure 2). The observed complexity of the amplitude patterns reflects the complexity of the depth function. However, the curves $0.1\,n^{-4}$ and $0.1\,n^{-2}$ bounding the maxima of the ER-amplitudes and the SR-amplitudes, respectively, remain practically the same. For the geometrical configurations examined in this work, extensive numerical evidence has shown that the most significant parameters

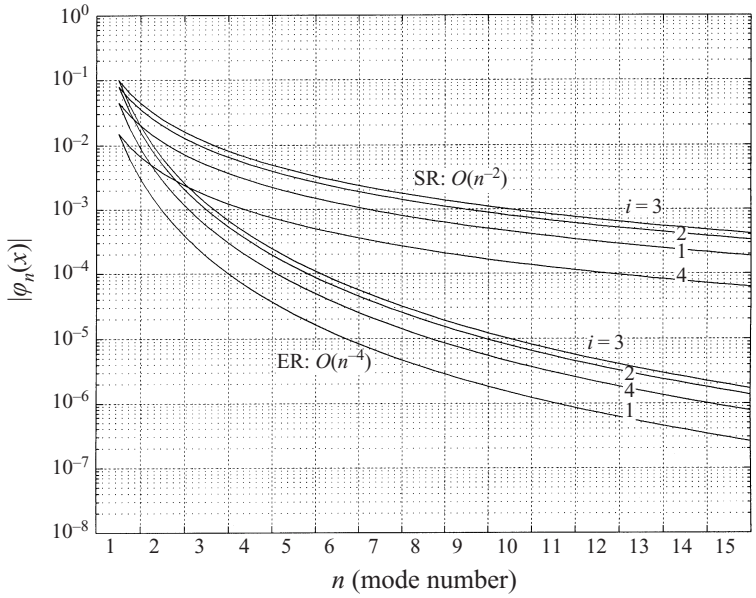

FIGURE 6. Bounding curves for the maximum moduli $\max|\varphi_n(x)|$ of the modal-amplitude functions *vs.* mode-number n, for four different frequencies, as obtained by the ER and the SR models. The values of the index $i = 1, 2, 3, 4$ correspond to the angular frequencies $\omega_1 = 0.5\,\mathrm{rad\,s^{-1}}$, $\omega_2 = 1\,\mathrm{rad\,s^{-1}}$, $\omega_3 = 2\,\mathrm{rad\,s^{-1}}$ and $\omega_4 = 4\,\mathrm{rad\,s^{-1}}$ respectively. The results of this figure apply to both depth functions given by equations (6.2) and (6.3).

Case i	$\omega_i(\mathrm{rad\,s^{-1}})$	T(s)	h_1/λ_1	h_3/λ_3	s_i(SR)	e_i(ER)
1	0.5	12.56	0.064	0.036	0.045	0.016
2	1.0	6.28	0.138	0.074	0.092	0.087
3	2.0	3.14	0.395	0.166	0.100	0.100
4	4.0	1.57	1.550	0.520	0.015	0.440

TABLE 2. Coefficients e_i and s_i of the bounding curves of the moduli $|\varphi_n(x)|$ of the modal amplitude functions.

controlling the modal-amplitude bounding curves are $h_1/\lambda_1, h_3/\lambda_3$ or, for a given geometry, the frequency ω. This situation is depicted in more detail in figure 6, where the curves bounding the maxima of the ER-amplitudes and the SR-amplitudes, respectively, are plotted *vs.* the mode number for four different frequencies ranging from $\omega = 0.5\,\mathrm{rad\,s^{-1}}$ (corresponding to shallow water conditions at both ends) to $\omega = 4\,\mathrm{rad\,s^{-1}}$ (corresponding to deep water conditions at both ends). The values of the parameters $h_1/\lambda_1, h_3/\lambda_3$, as well as the coefficients of the bounding curves e_i(ER) and s_i(SR) are given in table 2. In figure 6 (and also table 2) we can observe that as $h_1/\lambda_1, h_3/\lambda_3$ either increase (towards and above the deep water limit: $h/\lambda \approx 0.5$) or decrease (towards and below the shallow water limit: $h/\lambda \approx 0.07$) the coefficients of the bounding curves decrease, while the exponents (controlling the rate of decay) remain unaltered. Thus, we can conclude that the rate of decay is characteristic of the type (ER or SR) of the representation used. (Of course, the general validity of this statement has to be supported by a mathematical proof.) Another interesting result that can be seen in figure 6 is that the weaker bound (i.e. the bounding curves $i = 2, 3$)

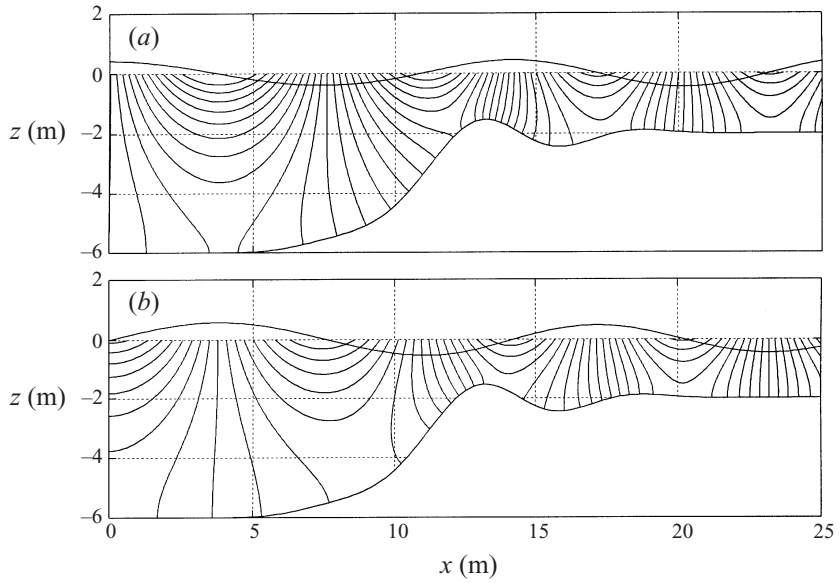

FIGURE 7. The same as figure 4, but for the depth function given by equation (6.3).

occurs, for both representations, when the shallowness parameters are in the range of intermediate water depth, i.e. when $0.07 < h_1/\lambda_1, h_3/\lambda_3 < 0.5$. The results of figures 5 and 6 (and also of figure 2) demonstrate the superiority of the present method concerning both the rate of convergence and the practical usefulness of the enhanced representation of the wave field. It can be clearly seen that, when the sloping-bottom mode is included, a small number of evanescent modes is sufficient to obtain accurate results, even in environments with complex bottom geometry.

Moreover, the present analysis permits us to obtain uniformly valid numerical bounds for the error of the calculated wave potential, by both the ER model and the SR model. Indeed, the numerically established bounds of the form $|\varphi_n(x;\omega)| \leqslant e(\omega)n^{-4}$ for ER, and $|\varphi_n(x;\omega)| \leqslant s(\omega)n^{-2}$ for SR, imply the error bounds

$$E_{ER}(N_e) = \frac{gH}{2\omega}\left|\sum_{n=N_e+1}^{\infty}\varphi_n(x)Z_n(z;x)\right| \leqslant \frac{gH}{2\omega}e(\omega)Z(\omega)\sum_{n=N_e+1}^{\infty}n^{-4}, \tag{6.4a}$$

$$E_{SR}(N_e) = \frac{gH}{2\omega}\left|\sum_{n=N_e+1}^{\infty}\varphi_n(x)Z_n(z;x)\right| \leqslant \frac{gH}{2\omega}s(\omega)Z(\omega)\sum_{n=N_e+1}^{\infty}n^{-2}, \tag{6.4b}$$

where $Z(\omega) = \max\{|Z_n(z;x)|, a \leqslant x \leqslant b, -h(x) \leqslant z \leqslant 0\}$. For example, for $\omega = 2\,\mathrm{rad\,s^{-1}}$ and $H = 1\,\mathrm{m}$ ($Z(\omega) = 1.45$ in this case), the absolute errors (relative errors defined with respect to the maximum absolute value of the wave potential in the variable bathymetry region) in the field calculation when only $N_e = 3$ evanescent modes are used are $E_{ER}(3) = 0.0026\,\mathrm{m^2\,s^{-1}}(0.1\%)$ and $E_{SR}(3) = 0.1009\,\mathrm{m^2\,s^{-1}}(3.5\%)$. (In this case $e(\omega) = s(\omega) = 0.1$; see also table 2.) When $N_e = 6$ evanescent modes are retained the corresponding errors become $E_{ER}(6) = 0.0004\,\mathrm{m^2\,s^{-1}}(0.01\%)$ and $E_{SR}(6) = 0.055\,\mathrm{m^2\,s^{-1}}(2\%)$.

In figure 7 the equipotential lines of the wave field (real and imaginary part) in the variable bathymetry subdomain $D^{(2)}$, obtained by the ER model with $N_e = 6$ evanescent modes, are presented. Also in the same figure the free-surface elevation

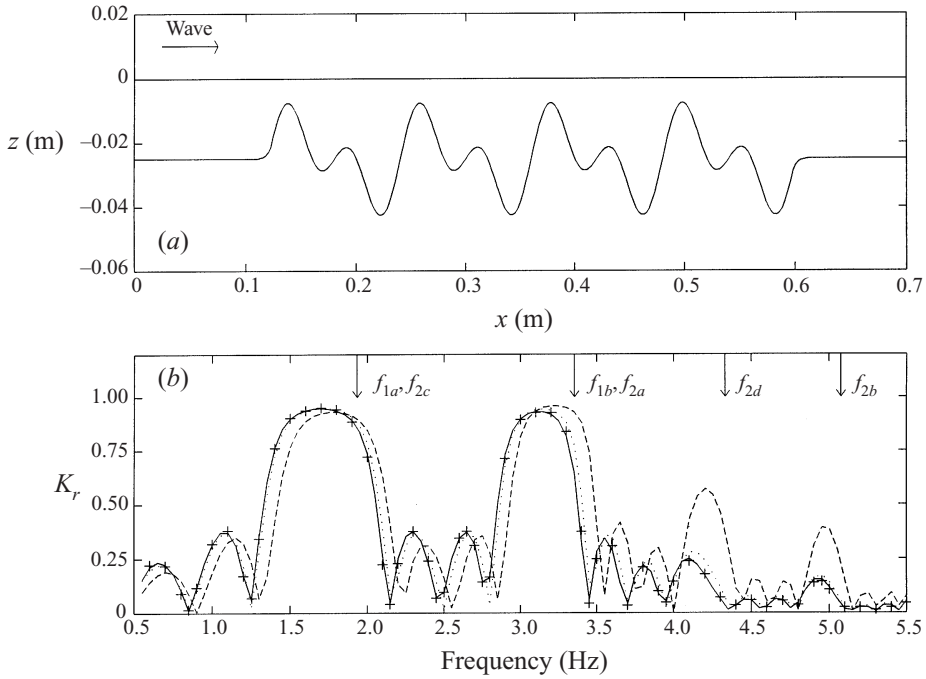

FIGURE 8. (*a*) Geometrical configuration of the doubly periodic bed specified by equation (6.5). (*b*) Reflection coefficient (K_r) *vs.* frequency. Numerical results shown have been obtained by using ——, the ER model, ·····, the SR model and – – –, the MMS model. ×, numerical results obtained by Guazzelli *et al.* (1992). The first-order and the second-order Bragg resonance frequencies ($f_{1\cdot}$ and $f_{2\cdot}$, respectively) are indicated by arrows.

is shown for $H = 1\,\text{m}$. The wave pattern is again very satisfactory, and the ER equipotential lines intersect the bottom profile perpendicularly, as expected. The corresponding SR-equipotential lines (not shown in the figure) exhibit the same inconsistency as before, i.e. near the bottom they bend and become vertical at $z = -h(x)$; (cf. figure 4).

6.2.3. *The case of a doubly periodic bed*

As a last example we consider a doubly sinusoidal bed profile which has been extensively studied by Mei (1985) and Guazzelli, Rey & Belzons (1992), in connection with Bragg scattering. The bottom geometry is defined by (see also figure 8*a*)

$$h_b(x) = \begin{cases} 2.5\,\text{cm}, & x \leqslant 12\,\text{cm} \\ 2.5 - \sin(K_1(x-12)) - \sin(K_2(x-12))\,\text{cm}, & 12\,\text{cm} < x < 60\,\text{cm} \\ 2.5\,\text{cm}, & x \geqslant 60\,\text{cm}, \end{cases} \tag{6.5}$$

where $K_1 = 0.52\,\text{cm}^{-1}$ and $K_2 = 1.05\,\text{cm}^{-1}$ are the wavenumbers of the bed profile. Because of the specific interest in resonance reflections, in this case we focus on the variation of the reflection coefficient $K_r = |A_R|/|A_0|$ *vs.* frequency, which is presented in figure 8(*b*). Numerical results have been obtained by means of the ER model (using the propagating, the sloping-bottom and 3 evanescent modes), the SR model (excluding the sloping-bottom mode) and the MMS model (excluding also all evanescent modes). In all cases, $N = 201$ points have been used for the discretization

of the variable bathymetry domain. In the same figure, numerical results are also plotted (shown by crosses), obtained by Guazzelli *et al.* (1992) by means of the method of stepwise approximation with 3 evanescent modes.

In the studied case, the first-order Bragg resonances, corresponding to $0.5K_1$ and $0.5K_2$, occur at the frequencies $f_{1a} = 1.93$ Hz and $f_{1b} = 3.35$ Hz, respectively. The second-order Bragg resonance, corresponding to K_1, K_2, $0.5(K_2 - K_1)$ and $0.5(K_2 + K_1)$, occur at the frequencies $f_{2a} = 3.35$ Hz, $f_{2b} = 5.07$ Hz, $f_{2c} = 1.93$ Hz and $f_{2d} = 4.33$ Hz, respectively. The results obtained by using the ER and the SR models seem, in general, to be comparable; however, there exists a frequency shifting, creating discrepancies in some frequency ranges (e.g. 1.9–2.2 Hz, 3.25–3.4 Hz, 4.2–4.35 Hz). The reflection coefficient calculated by the MMS model is more shifted towards higher frequencies, resulting to significant discrepancies in broader frequency intervals (e.g. 3.3–3.7 Hz, 4.1–4.4 Hz). In addition, it can be observed in figure 8(*b*) that the MMS-model predictions of the reflection coefficient differs significantly from those of all other methods in the neighbourhood of the second-order Bragg resonance frequencies.

The results obtained by the ER model are in excellent agreement with those obtained by the method of stepwise approximation. This is expected since both methods treat the complete linear problem, i.e. they do not introduce any simplifying assumptions concerning the bottom boundary. However, an important difference between the two methods lies in the calculation of the velocity field near and on the bottom surface. While the ER model can predict a smooth and realistic approximation of the tangential bottom velocity, the stepwise approximation technique introduces artificial corners rendering the wave velocity locally singular.

7. Concluding remarks

A consistent coupled-mode theory has been derived for the propagation of small-amplitude water waves over variable bathymetry regions. The present method does not introduce any simplifying assumptions or other restrictions concerning either the bottom slope and curvature, or the vertical structure of the wave field. All wave phenomena (refraction, reflection, diffraction) are fully modelled and, thus, the present method can serve as a useful tool for the analysis of the wave field in the whole range of parameters within the regime of linear theory.

Technically, the key feature of the present method is the introduction of an additional mode, completely describing the influence of the bottom slope. It turns out that the presence of the additional mode in the series representation of the potential makes it consistent with the bottom boundary condition and, at the same time, substantially accelerates the convergence. The obtained coupled-mode system of horizontal equations, being fully equivalent to any other complete linear model, presents a number of advantages as: (i) A few modes are sufficient to accurately calculate the wave field in the whole liquid domain. Thus, this method effectively treats the non-local character of the problem in the propagation space, identifying and retaining the most important couplings. (ii) The enhanced coupled-mode system can be naturally simplified either to the extended mild-slope equation or to the modified one in subareas where the physical conditions permit it. (iii) The present method provides high-quality information concerning the pressure and the tangential velocity at the bottom, which is useful for the study of oscillating bottom boundary layer and wave-energy dissipation, as well as for sea-bed movement and sediment transport studies. (iv) Because of the completeness of the representation of the velocity field, it can be used for the construction and the efficient numerical treatment of the corresponding Green's

function, which is the main tool for studying wave–body interaction problems in variable bathymetry regions. First results in this direction have been presented by Athanassoulis & Belibassakis (1997).

Finally, the analytical structure of the present model facilitates its extension to various directions as, e.g. to three-dimensional problems, to wave-current systems or to the weakly nonlinear (second- and higher-order) wave interactions in a variable bathymetry region. In all cases, the dissipation of wave energy can be approximately taken into account by including an appropriate imaginary part in the wavenumber, as in the case of the mild-slope equation (see, e.g. Dingemans 1997 and the references therein).

The authors are indebted to the referees for their constructive comments which helped them to improve some points in the presentation and motivated additional investigation on the effect of the various choices of $Z_{-1}(z;x)$. This work was partially supported by OCEANOR – Oceanographic Company of Norway ASA, in the framework of the POSEIDON/Aegean Sea project.

REFERENCES

Aranha, J. A., Mei, C. C. & Yue, D. K. P. 1979 Some properties of a hybrid element method for water waves. *Intl J. Numer. Meth. Engng* 1627–1641.

Athanassoulis, G. A. & Belibassakis, K. A. 1997 Water wave Green's function for a 3D uneven bottom problem with different depths at $x \to +\infty$ and $x \to -\infty$. *Proc. IUTAM Symp. on Computational Methods for Unbounded Domains*, 27–31 July 1997. University of Colorado at Boulder, pp. 21–32. Kluwer.

Athanassoulis, G. A. & Makrakis, G. N. 1994 A function-theoretic approach to a two-dimensional transient wave–body interaction problem. *Applicable Anal.* **54**, 283–303.

Bai, K. J. & Yeung, R. W. 1974 Numerical Solution to free-surface flow problems. *Proc. 10th Naval Hydrodyn. Symp.* Office of Naval Research, Cambridge, MA, 1974, pp. 609–641.

Berkhoff, J. C. W. 1972 Computation of combined refraction–diffraction. *Proc. 13th Conf. Coastal Engng, Vancouver*, vol. 2, pp. 471–490. ASCE.

Berkhoff, J. C. W. 1976 Mathematical models for simple harmonic linear waves. Wave diffraction and refraction. PhD thesis, Technical University of Delft.

Berkhoff, J. C. W., Booij, N. & Radder, A. C. 1982 Verification of numerical wave propagation models for simple harmonic linear water waves. *Coastal Engng* **6**, 255–279.

Booij, N. 1981 Gravity waves on water with non-uniform depth and current. PhD thesis, Technical University of Delft.

Booij, N. 1983 A note on the accuracy of the mild-slope equation. *Coastal Engng* **7**, 191–203.

Boyles, C. A. 1984 *Acoustic Waveguides. Applications to Oceanic Science*. John Wiley.

Chamberlain, P. G. & Porter, D. 1995 The modified mild-slope equation. *J. Fluid Mech.* **291**, 393–407.

Coddington, E. A. & Levinson, N. 1995 *Theory of Ordinary Differential Equations*. McGraw-Hill, New York.

Craig, W. & Sulem, G. 1993 Numerical simulation of gravity waves. *J. Comput. Phys.* **108**, 73–83.

Davies, A. G. & Heathershaw, A. D. 1984 Surface-wave propagation over sinusoidal varying topography. *J. Fluid Mech.* **291**, 419–433.

Devillard, P., Dunlop, F. & Souillard, B. 1988 Localization of gravity waves on a channel with a random bottom. *J. Fluid Mech.* **186**, 521–538.

Dingemans, M. 1997 *Water Wave Propagation over Uneven Bottoms*. World Scientific.

Eckart, G. 1952 The propagation of gravity waves from deep to shallow water. In *Gravity Waves: Proc. NBS Semicentennial Symp. on Gravity Waves, 15–18 June 1951*, pp. 156–175. Washington: National Bureau of Standards.

Euvrard, D., Jami, M., Lenoir, M. & Martin, D. 1981 Recent progress towards an optimal coupling

of finite elements and singularity distribution procedures in numerical ship hydrodynamics. *Proc. 3rd Intl Conf. on Numer. Ship Hydrodyn. Paris. June 1981*, pp. 193–210.

Evans, D. V. & Kuznetsov, C. M. 1997 *Gravity Waves in Water of Finite Depth* (ed. J. N. Hunt), ch. 4. Computational Mechanics Publications.

Evans, D. V. & Linton, C. M. 1994 On step approximations for water-wave problems. *J. Fluid Mech.* **278**, 229–249.

Fawcett, J. A. 1992 A derivation of the differential equations of coupled-mode propagation. *J. Acoust Soc. Am.* **92**, 290–295.

Fitz-Gerald, G. F. 1976 The reflexion of plane gravity waves travelling in water of variable depth. *Phil. Trans. R. Soc. Lond. Math. Phys. Sci.* **284**, 49–89.

Fitz-Gerald, G. F. & Grimshaw R. H. J. 1979 A note on the uniqueness of small-amplitude water waves travelling in a region of varying depth. *Math. Proc. Camb. Phil. Soc.* **86**, 511–519.

Garipov, R. M. 1965 Nonsteady waves above an underwater ridge. *Sov. Phys. Fluid Mech.* **10**, 194–196.

Gelfand, I. M. & Fomin, S. V. 1963 *Calculus of Variations*. Prentice-Hall.

Guazzelli E., Rey, V. & Belzons, M. 1992 Higher-order Bragg reflection of gravity surface waves by periodic beds. *J. Fluid Mech.* **245**, 301–317.

Hara, T. & Mei, G. C. 1987 Bragg scattering by periodic bars: theory and experiment. *J. Fluid Mech.* **178**, 221–241.

Higgins, J. R. 1977 *Completeness and Basis Properties of Sets of Special Functions*. Cambridge University Press.

Kirby, J. T. 1986*a* A general wave equation for waves over rippled beds. *J. Fluid Mech.* **162**, 171–186.

Kirby, J. T. 1986*b* On the gradual reflection of weakly nonlinear Stokes waves in regions with varying topography. *J. Fluid Mech.* **162**, 187–209.

Kuznetsov, N. G. 1991 Uniqueness of a solution of a linear problem for stationary oscillations of a fluid. *Diff. Eqns* **27**, 187–194.

Kuznetsov, N. G. 1993 The Maz'ya identity and lower estimates of eigenfrequencies of steady-state oscillations of a liquid in a channel. *Russian Math. Surveys* **48**, 222.

Lenoir, M. & Tounsi, A. 1988 The localized finite element method and its application to the two-dimensional sea-keeping problem. *SIAM J. Numer. Anal.* **25**, 729–752.

Lozano, C. & Meyer, R. E. 1976 Leakage and response of wave-trapped by round islands. *Phys. Fluids* **19**, 1075–1088.

Massel, S. 1989 *Hydrodynamics of Coastal Zones*. Elsevier.

Massel, S. 1993 Extended refraction–diffraction equations for surface waves. *Coastal Engng* **19**, 97–126.

Mei, C. C. 1978 Numerical methods in water-wave diffraction and radiation. *Ann. Rev. Fluid Mech.* **10**, 393–416.

Mei, C. C. 1983 *The Applied Dynamics of Ocean Surface Waves*. John Wiley (2nd reprint, 1994, World Scientific).

Mei, C. C. 1985 Resonant reflection of surface waves by periodic sandbars. *J. Fluid Mech.* **152**, 315–335.

Mei, C. C. & Black, J. L. 1969 Scattering of surface waves by rectangular obstacles in waters of finite depth. *J. Fluid Mech.* **38**, 499–511.

Mei, C. C. & Chen, H. S. 1975 Hybrid element method for water waves. *Proc. Symp. Modeling Techniques, 2nd Ann. Symp. of the Waterways Harbors and Coastal Engng*, vol. 1, pp. 63–81. ASCE.

Mei, C. C. & Chen, H. S. 1976 A hybrid element method for steady linearized free surface flows. *Intl J. Numer Meth. Engng* **10**, 1153–1175.

Milder, M. D. 1977 A note on Hamilton's principle for surface waves. *J. Fluid Mech.* **83**, 159–161.

Miles, J. W. 1967 Surface-wave scattering matrix for a shelf. *J. Fluid Mech.* **28**, 755–767.

Miles, J. W. 1977 Hamilton's principle for surface waves. *J. Fluid Mech.* **83**, 153–158.

Miles, J. W. 1991 Variational approximations for gravity waves of variable depth. *J. Fluid Mech.* **232**, 681–688.

Moiseev, N. N. 1964 Introduction to the theory of oscillations of liquid containing bodies. *Adv. Appl. Maths* **3**, 233–289.

Moiseev, N. N. & Rumiantsev, V. V. 1968 *Dynamic Stability of Bodies Containing Fluid*. Springer.

NEWMAN, J. N. 1965 Propagation of water waves over an infinite step. *J. Fluid Mech.* **23**, 399–415.

O'HARE, T. J. & DAVIES, A. G. 1992 A new model for surface wave propagation over undulating topography. *Coastal Engng* **19**, 251–266.

O'HARE, T. J. & DAVIES, A. G. 1993 A comparison of two models for surface-wave propagation over rapidly varying topography. *Appl. Ocean Res.* **15**, 1–12.

PIERCE, A. D. 1965 Extension of the method of normal modes to sound propagation in an almost-stratified medium. *J. Acoust. Soc. Am.* **37**, 19–27.

PORTER, D. & CHAMBERLAIN, P. G. 1997 Linear wave scattering by two-dimensional topography. *Gravity Waves in Water of Finite Depth* (ed. J. N. Hunt), ch. 2. Computational Mechanics Publications.

PORTER, D. & STAZIKER, D. J. 1995 Extension of the mild-slope equation. *J. Fluid Mech.* **300**, 367–382.

RADDER, A. G. & DINGEMANS, M. W. 1985 Canonical equations for almost periodic, weakly nonlinear gravity waves. *Wave Motion* **7**, 473–485.

REKTORYS, K. 1977 *Variational Methods in Mathematics.* D. Reidel.

REY, V. 1992 Propagation and local behaviour of normal incident gravity waves over varying topography. *Eur. J. Mech.* B: *Fluids* **11**, 213–232.

RUTHERFORD S. R. & HAWKER K. E. 1981 Consistent coupled mode theory of sound propagation for a class of nonseparable problems. *J. Acoust. Soc. Am.* **70**, 554–584.

SIMON, M. J. & URSELL, F. 1984 Uniqueness in linearized two-dimensional water-wave problems. *J. Fluid Mech.* **148**, 137–154.

SMITH, R. & SPRINKS, T. 1975 Scattering of surface waves by conical island. *J. Fluid Mech.* **72**, 373–384.

STOKER, J. J. 1957 *Water Waves.* Interscience.

TITCHMARSH, E. G. 1962 *Eigenfunction Expansions*, 2nd edn. Clarendon.

VAINBERG, B. R. & MAZ'JA, V. G. 1973 On the problem of steady state oscillations of a fluid layer of variable depth. *Trans. Moscow Math. Soc.* **28**, 56–73.

VOLTERRA, V. 1929 *Theory of Functionals and of Integral and Integrodifferential Equations.* Blackie (republished 1959, Dover).

WEHAUSEN, J. N. & LAITONE, E. V. 1960 *Surface Waves.* Handbuch der Physik. Springer.

YEUNG, R. W. 1982 Numerical methods in free-surface flows. *Ann. Rev. Fluid Mech.* **14**, 395–442.